EANAM10, September 15-19, 2025 https://coma.kasi.re.kr/eanam10/program/

Multi-component-abundance-isotope SEPs acceleration by coupled hydrodynamic,magnetodynamic, and kinetic processes in fractal current sheets in solar flare/CMES

Bojing Zhu(朱伯靖)

Yunnan Observatories & Center for Astronomical Mega-Science of CAS(bjzhu@ynao.ac.cn)
Earth and Planetary College & School of Astronomy and Space Science, UCAS (cynosureorion@ucas.ac.cn)
Sciences, State Key Laboratory of Space Weather, National Space Science Center, CAS
Yunnan Key Laboratory of Solar Physics and Space Science

Cooperate with

Yongbing Li, Yang Zhao, Qian Wang: Earth and Planetary College, University of Chinese Academy of Sciences

Yan Li, Zhikuo Ma, Zehua Fu,Zhihe Wang: Yunnan Observatories; Yunnan Key Laboratory of Solar Physics and Space Science.

Hui Yan,Ying Zhong: National Supercomputer Center in Guangzhou, Sun Yat-sen University **(Tianhe-2 CPU)**

Wu Wang, Yufeng Guo, Qing Ji: National Supercomputer Center in CAS, CNIC **(Dongfang seriers, CPU-DCU)**

Chunye Gong, Gang Zheng, Chuan Wang: National Supercomputer Center in Tianjin &National University of Defense Technology **(CPU-ARM)**

Acknowledge

(CU Boulder) George Ignatius Fann (OKA)、Robert von Fay-Siebenburgen(UOS)、 Hua-Liang Wei(UOS)、Matthew Gregg Knepley (
Mark F Adams(LBNL)、Hui Li(LANL) 、Shengtai Li(LANL)、David A Yuen(CU) et.al

15:00-15:20 SEP 17, 2025

OUTLINE

1. Background and Motivation

What & Why, Research progress, Science points, How- Key points

2. RHPIC-LBM: X86CPU & CPU-GPU & CPU-DCU &ARMCPU

Method, Algorithm, code, validation

3. Application (Events Study)

3D turbulence acceleration[source and origin, Electron, Proton, 3He, 4He;3He rich]

4. Summary and Future Works

Traditional turbulence acceleration(1st & 2nd Fermi) and wave-particle interaction acceleration
Other heavy particles & Different ionization states

1. Background and Motivation

What & Why: GeV-level-SEPs space weather disasters vs. source-origin(Heavy particle, 3He rich)

Research progress: Supercomputer(SUGON,TIANHE-3) & observational data(FY-3E heavy SEPs)

How- Science points: Multi-component-abundance-isotope, Turbulence induced viscosity & resistivity dissipation and diffusion

Key points: 3D turbulence MR, 3D topologies evolution, Fractal CS mode

Motivation: SEPs induced extremely space weather disasters

GeV-level-SEPs-induced extreme space weather disasters. **identifying producing source and origin**

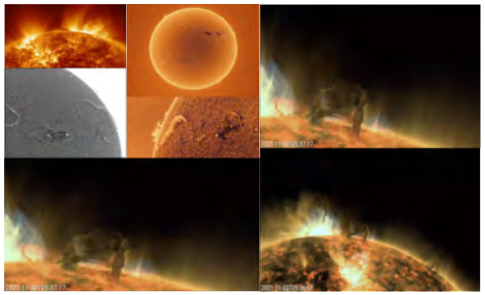

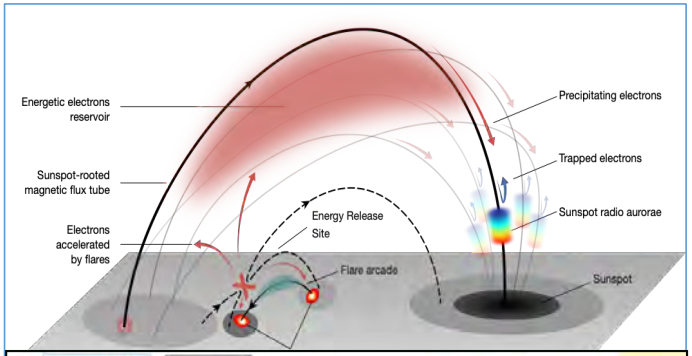

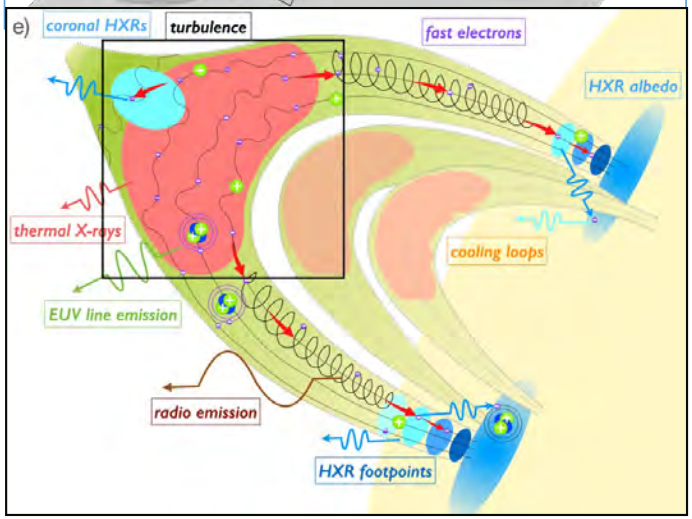

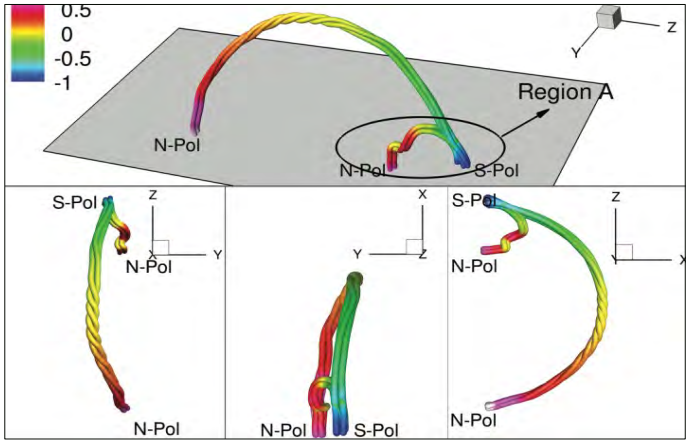

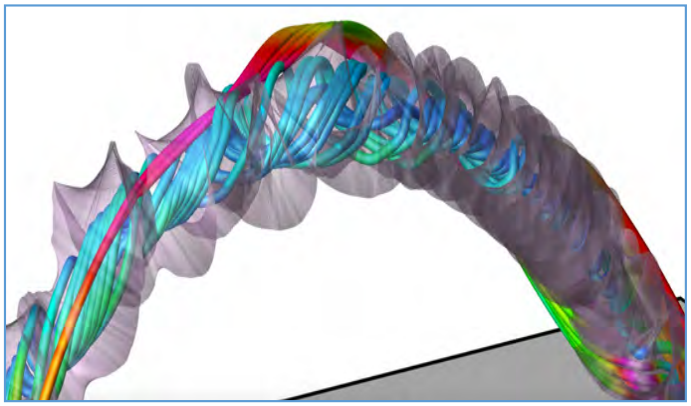

Research progress : Supercomputer & Observational data

Our research team: Early warning system of SEPS-induced space weather disasters with the observational data-driven multi-component-abundance-isotope model through plasma statistical physics theoretical framework on the domestic supercomputer

FY-3E SEPs Observational data

SUGON Heterogeneous DCU(NSCC-CAS) 2019 ~

ARM CPU TIANHE-3(NUDT&NSCC-TJ) 2023 ~

CPU TIANHE-2(NUDT&NSCC-GZ) 2014 ~

Science points: Multi-components, multi-abundance, multi-isotope


Journal Pre-proofs

Review of Solar Energetic Particle Models

Kathryn Whitman, Ricky Egeland, Ian G. Richardson, Clayton Allison, Philip Quinn, Janet Barzilla, Irina Kitiashvili, Viacheslav Sadykov, Hazel M. Bain, Mark Dierckxsens, M. Leila Mays, Tilaye Tadesse, Kerry T. Lee, Edward Semones, Janet G. Luhmann, Marlon Núñez, Stephen M. White, Stephen W. Kahler, Alan G. Ling, Don F. Smart, Margaret A. Shea, Valeriy Tenishev, Soukaina F. Boubrahimi, Berkay Aydin, Petrus Martens, Rafal Angryk, Michael S. Marsh, Silvia Dalla, Norma Crosby, Nathan A. Schwadron, Kamen Kozarev, Matthew Gorby, Matthew A. Young, Monica Laurenza, Edward W. Cliver, Tommaso Alberti, Mirko Stumpo, Simone Benella, Athanasios Papaioannou, Anastasios Anastasiadis, Ingmar Sandberg, Manolis K. Georgoulis, Anli Ji, Dustin Kempton, Chetraj Pandey, Gang Li, Junxiang Hu, Gary P. Zank, Eleni Lavasa, Giorgos C[illegible], Yash Kadadi, Ian Fernandes, Maher A. Du[illegible], Subhamoy Chatterjee, Kimberly D. Morel[illegible], Roussev, Aleksandre Taktakishvili, Freder[illegible], Zhenguang Huang, Lulu Zhao, Nicolas W[illegible], Athanasios Kouloumvakos, Miikka Paassilita, Rami Vainio, Anatoly Belov, Eugenia A. Eroshenko, Maria A. Abunina, Artem A. Abunin, Christopher C. Balch, Olga Malandraki, Michalis Karavolos, Bernd Heber, Johannes Labrenz, Patrick Kühl, Alexander G. Kosovichev, Vincent Oria, Gelu M. Nita, Egor Illarionov, Patrick M. O'Keefe, Yucheng Jiang, Sheldon H. Fereira, Aatiya Ali, Evangelos Paouris, Sigiava Aminalragia-Giamini, Piers Jiggens, Meng Jin, Christina O. Lee, Erika Palmerio, Alessandro Bruno, Spiridon Kasapis, Xiantong Wang, Yang Chen, Blai Sanahuja, David Lario, Carla Jacobs, Du Toit Strauss, Ruhann Steyn, Jabus den Berg van, Bill Swalwell, Charlotte Waterfall, Mohamed Nedal, Rositsa Miteva, Momchil Dechev, Pietro Zucca, Alec Engell, Brianna Maze, Harold Farmer, Thuha Kerber, Ben Barnett, Jeremy Loomis, Nathan Grey, Barbara J. Thompson, Jon A. Linker, Ronald M. Caplan, Cooper Downs, Tibor Török, Roberto Lionello, Viacheslav Titov, Ming Zhang, Pouya Hosseinzadeh

PII: S0273-1177(22)00724-4
DOI: https://doi.org/10.1016/j.asr.2022.08.006
Reference: JASR 16144

ADVANCES IN SPACE RESEARCH

Please cite this article as: Whitman, K., Egeland, R., Richardson, I.G., Allison, C., Quinn, P., Barzilla, J., Kitiashvili, I., Sadykov, V., Bain, H.M., Dierckxsens, M., Leila Mays, M., Tadesse, T., Lee, K.T., Semones, E., Luhmann, J.G., Núñez, M., White, S.M., Kahler, S.W., Ling, A.G., Smart, D.F., Shea, M.A., Tenishev, V., Boubrahimi, S.F., Aydin, B., Martens, P., Angryk, R., Marsh, M.S., Dalla, S., Crosby, N., Schwadron, N.A., Kozarev, K., Gorby, M., Young, M.A., Laurenza, M., Cliver, E.W., Alberti, T., Stumpo, M., Benella, S., Papaioannou, A., Anastasiadis, A., Sandberg, I., Georgoulis, M.K., Ji, A., Kempton, D., Pandey, C., Li, G., Hu, J., Zank, G.P., Lavasa, E., Giamnopoulos, G., Falconer, D., Kadadi, Y., Fernandes, I., Dayeh, M.A., Muñoz-Jaramillo, A., Chatterjee, S., Moreland, K.D., Sokolov, I.V., Roussev, I.I., Taktakishvili, A., Effenberger, F., Gombosi, T., Huang, Z., Zhao, L., Wijsen, N., Aran, A., Poedts, S., Kosdoumvakos, A., Paassilita, M., Vainio, R., Belov, A., Eroshenko, E.A., Abunina, M.A., Abunin, A.A., Balch, C.C., Malandraki, O., Karavolos, M., Heber, B., Labrenz, J., Kühl, P., Kosovichev, A.G., Oria, V., Nita, G.M., Illarionov, E., O'Keefe, P.M., Jiang, Y., Fereira, S.H., Ali, A., Paouris, E., Aminalragia-Giamini, S., Jiggens, P., Jin, M., Lee, C.O., Palmerio, E., Bruno, A., Kasapis, S., Wang, X., Chen, Y., Sanahuja, B., Lario, D., Jacobs, C., Strauss, D.T., Steyn, R., den Berg, J. van, Swalwell, B., Waterfall, C., Nedal, M., Miteva, R., Dechev, M., Zucca, P., Engell, A., Maze, B., Farmer, H., Kerber, T., Barnett, B., Loomis, J., Grey, N., Thompson, B.J., Linker, J.A., Caplan, R.M., Downs, C., Török, T., Lionello, R., Titov, V., Zhang, M., Hosseinzadeh, P., Review of Solar Energetic Particle Models, *Advances in Space Research* (2022), doi: https://doi.org/10.1016/j.asr.2022.08.006

will undergo additional copyediting, typesetting and review before it is published in its final form, but we are providing this version to give early visibility of the article. Please note that, during the production process, errors may be discovered which could affect the content, and all legal disclaimers that apply to the journal pertain.

© 2022 Published by Elsevier B.V. on behalf of COSPAR.

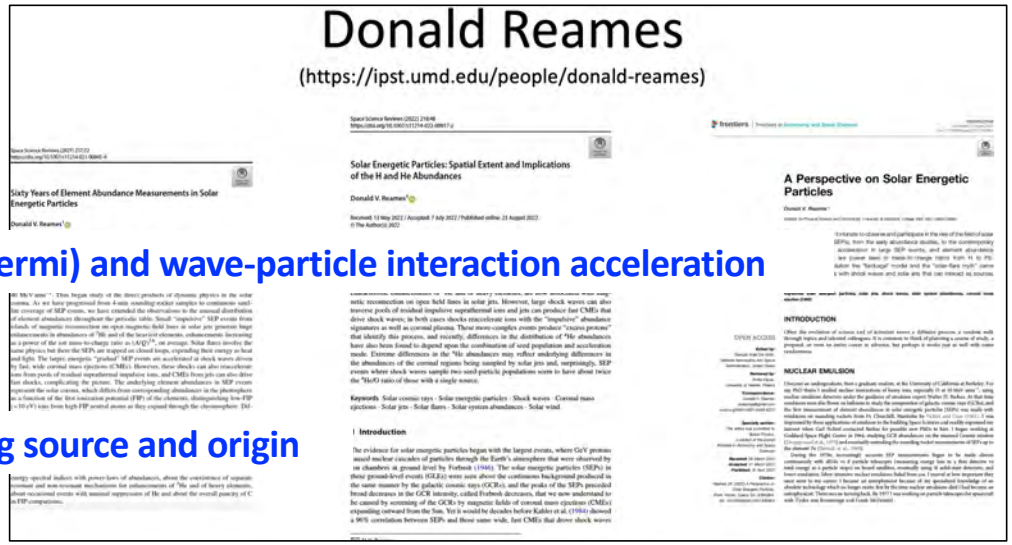
Donald Reames

(https://ipst.umd.edu/people/donald-reames)

Sixty Years of Element Abundance Measurements in Solar Energetic Particles

Donald V. Reames

Solar Energetic Particles: Spatial Extent and Implications of the H and He Abundances

Donald V. Reames

A Perspective on Solar Energetic Particles

Donald V. Reames

Traditional turbulence acceleration(1st & 2nd Fermi) and wave-particle interaction acceleration

identifying producing source and origin

Table 1. Chemical composition of the Sun

Chemical composition	Percent of the overall mass	Type
Hydrogen	**73%**	**Dominated**
Helium	25%	Dominated
Oxygen	0.8%	Metals
Carbon	0.36%	Metals
Iron	0.16%	Metals
Neon	0.12%	Metals
Nitrogen	0.09%	Metals
Silicon	0.07%	Metals
Magnesium	0.05%	Metals
Sulphur	0.04%	Metals
Others combined	0.04%	Metals

Other heavy particles & Different ionization states

Table 2. Layers of the Sun

Layers	Thickness (km)	Temperature (K)	Type
Core	150,000	10,000,000	Inertial layer
Convection Zone	180,000	500,000	Inertial layer
[illegible]	[illegible]	0	Outer layer, un-magnetized, weakly ionized
[illegible]	[illegible]	8000	Outer layer, magnetized, partly ionized [2]
Transition region	100	8000 – 500,000	Outer layer, magnetized, high ionized
Corona	5,000,000	1,000,000	Outer layer, magnetized, fully ionized

Science points: Fractal CS model

B&U decoupled condition and Fine structure investigation

Turbulence induced viscosity & resistivity dissipation and diffusion

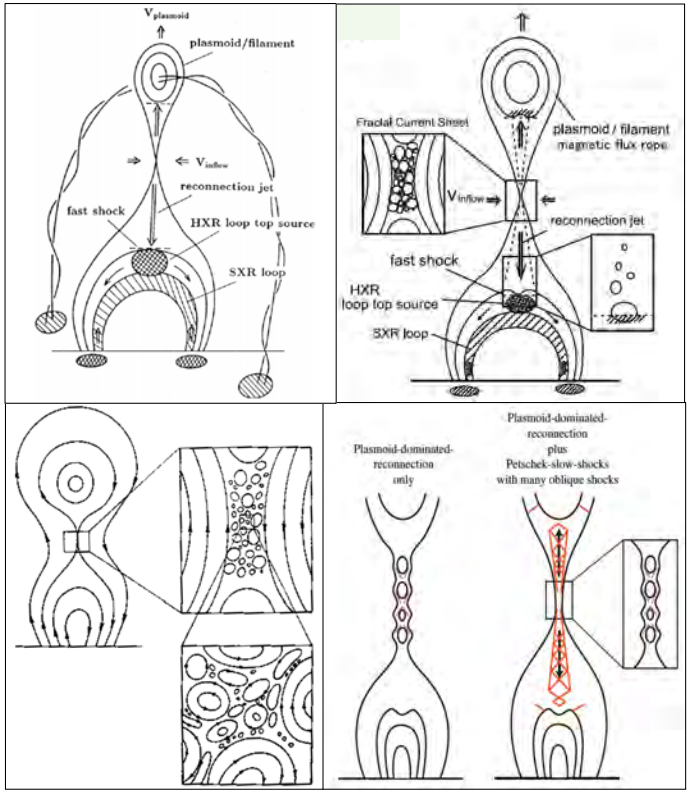

Shibata et al., 1995;,Tsuneta et al., 1992; Masuda et al., 1994; Tajima & Shibata 1997; Mann et al., 2006; Zenitani and Miyoshi 2011; Zenitani 2015

Theoretical Model from Observation

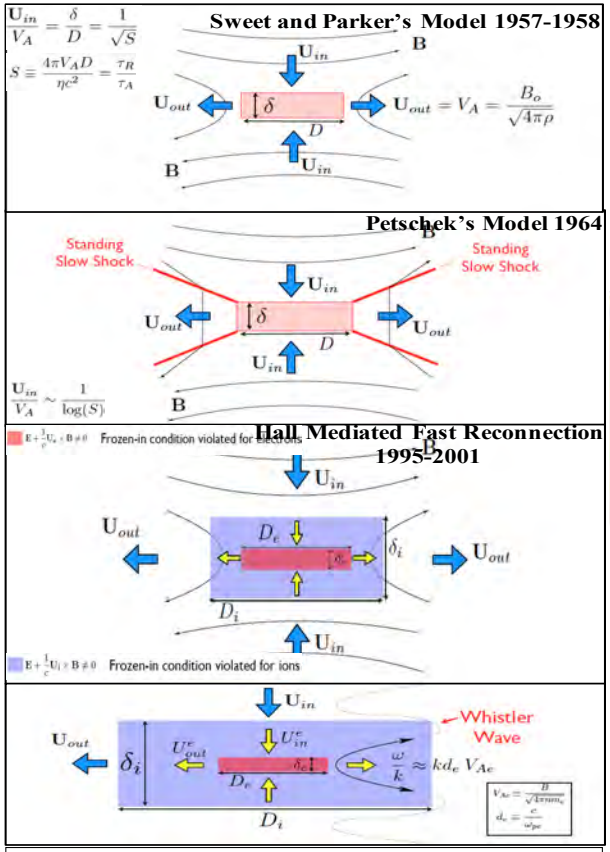

Theoretical Model from Plasma

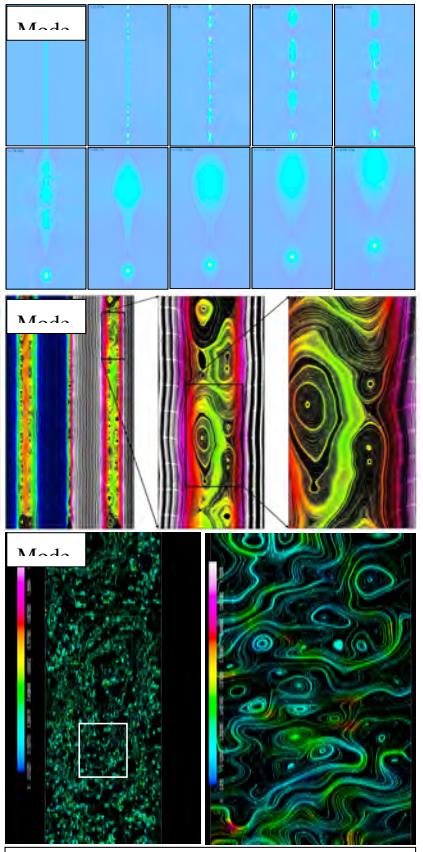

Numerical Model from Simulation

Model A: single current sheet?

Zenitani and Miyoshi (2011) and Zenitani (2015)

Model B: several current sheet?

D. Burgess, P. W. Gingell, and L. Matteini (2016)

Model C: full of kinetic scale current sheet?

Lazarian & Vishniac (1999), Servidio et al. (2009, 2010, 2011),G. P. Zank et al(2014

Key points: 3D turbulence MR

Turbulence plays a key role in the energy diffusion-dispersion-dissipation, flare heating and SEP energization and acceleration.

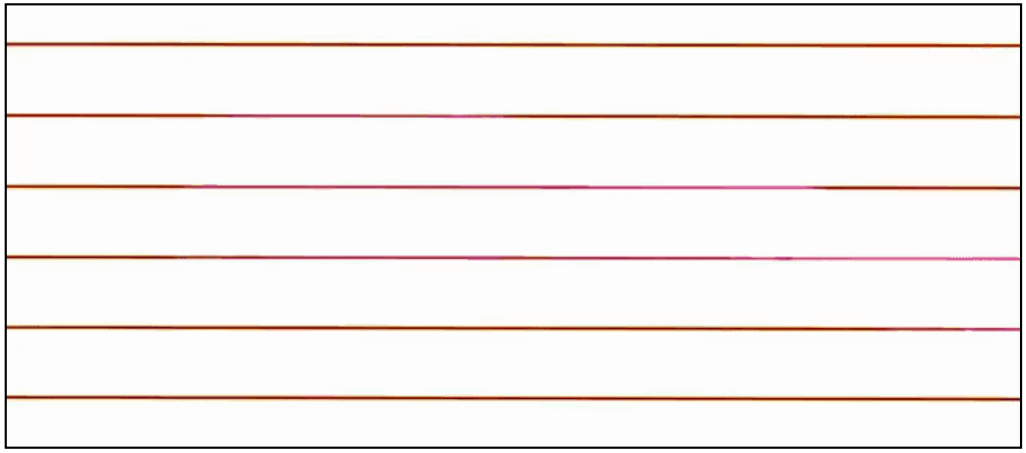

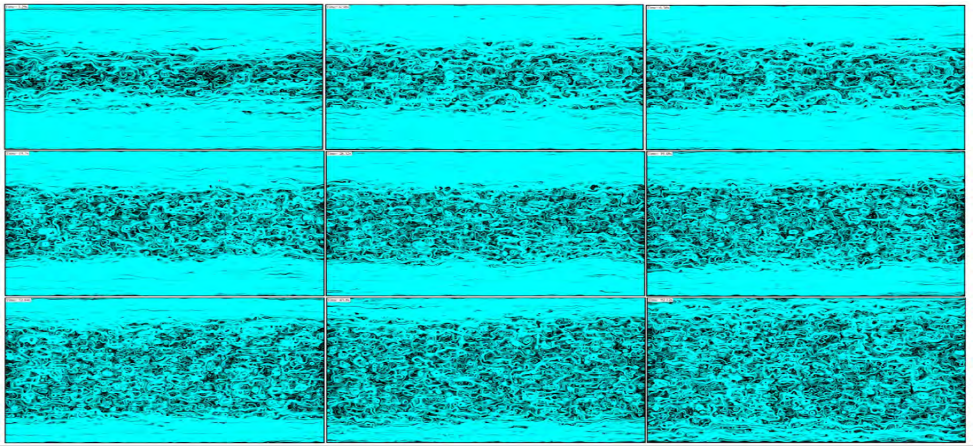

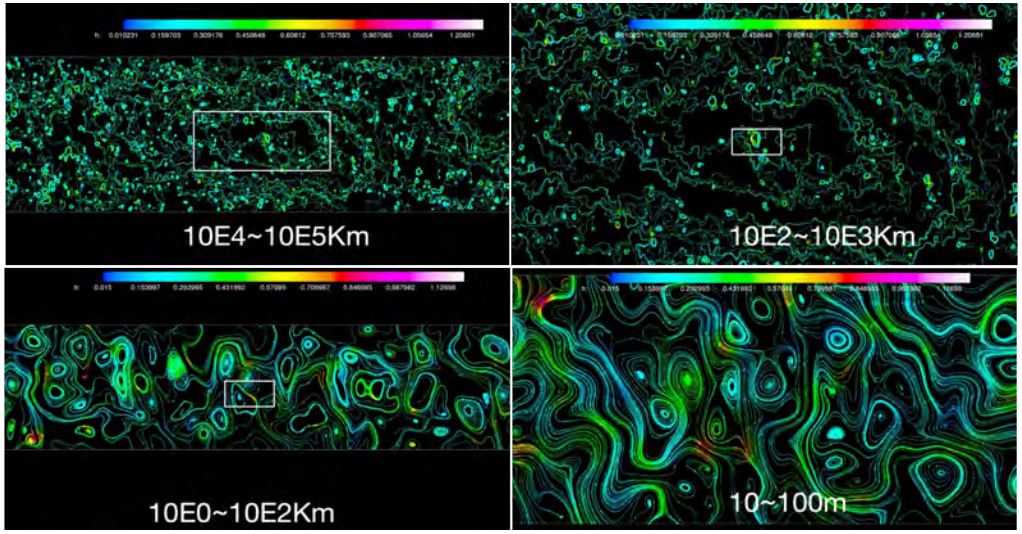

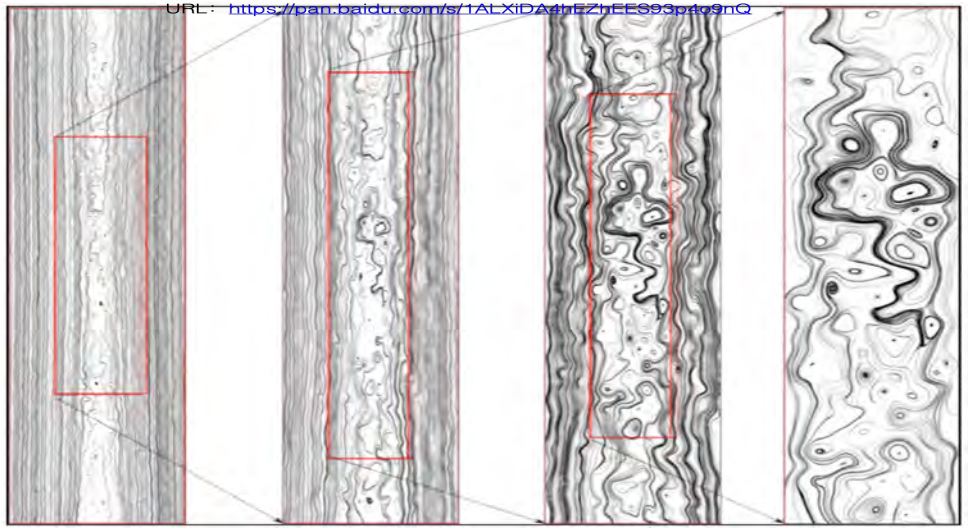

BOJING ZHU 2016 (Zhu et al 2019,2020a,2020b). Video URL: https://pan.baidu.com/s/1ALXiDA4hEZhEES93p4o9nQ

Key points: 3D turbulence MR

Fundamentally three-dimensional: What is hidden in the interim of the vorticity (plasma bubble; magnetic islands/magnetic helical structure)

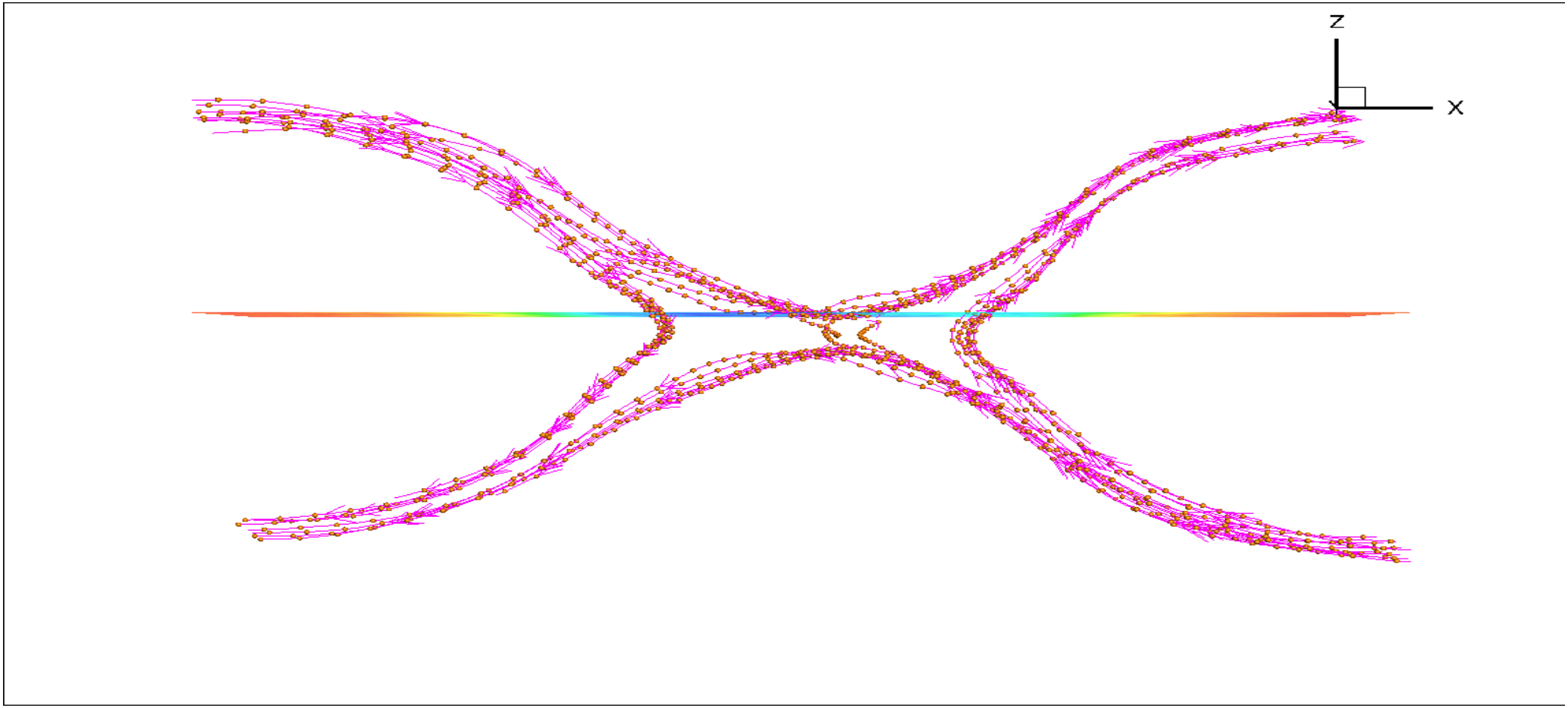

Birn and Priest 2007: Pontin 2011: Gonzales and Parker 2016: Zhu et al 2019.2020a.2020b:

Key points: 3D turbulence MR

Fundamentally three-dimensional: What is hidden in the interim of the vorticity (plasma bubble; magnetic islands/magnetic helical structure)

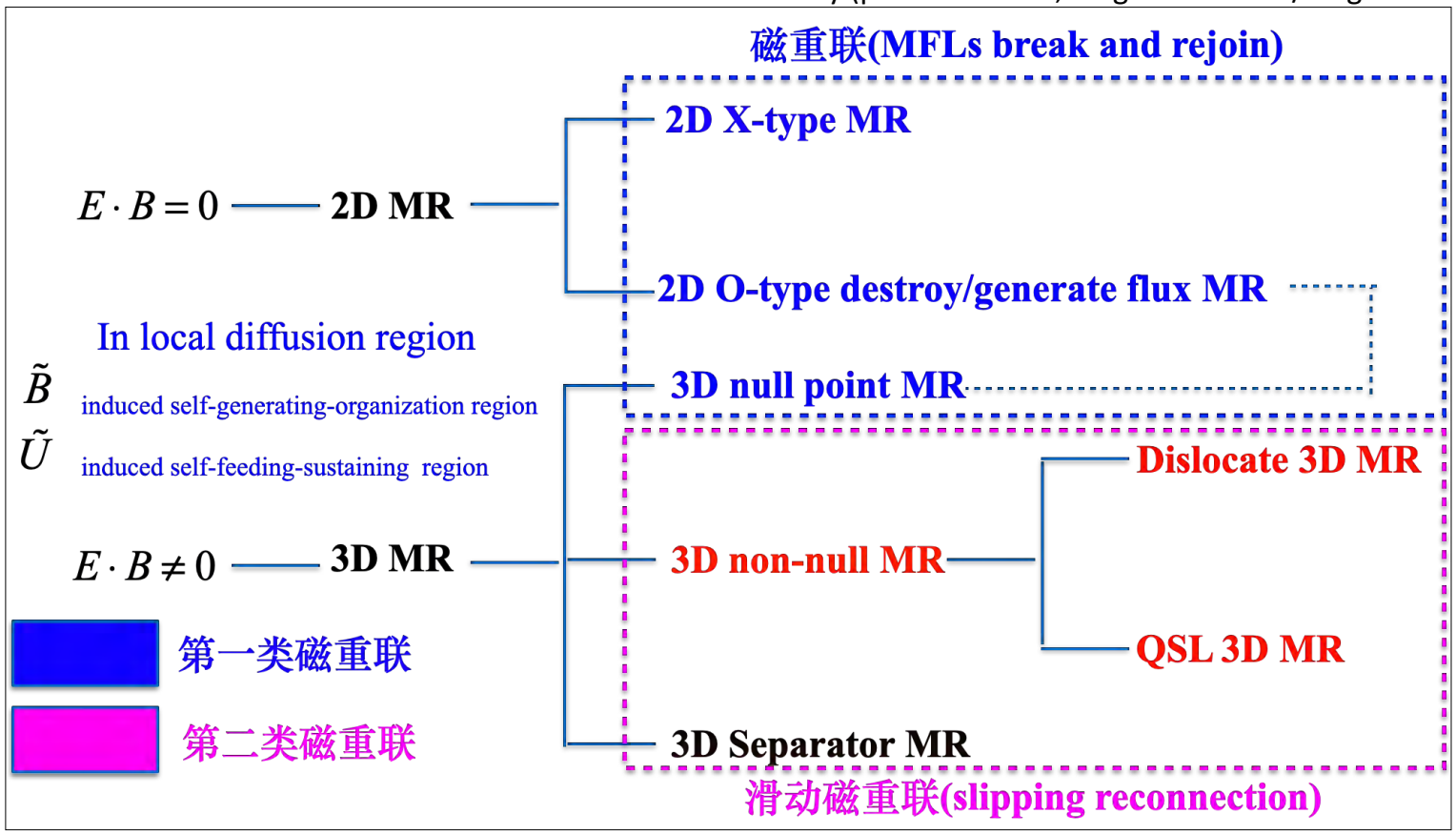

Magnetic islands: defined the **magnetic island** as a kind of magnetic field structure consisting of a bipolar magnetic field normal to the CS, with an enhancement of the core field in the axial direction with a compressed and high-temperature plasma inside of it.

Flux rope: Initial small magnetic helical perturbation will change the geometry and topology of the magnetic field, making MFLs orthogonal to the vector of the perturbation \tilde\bm B, forming a magnetic helical structure upon the flux surface (consisting of many spiral MFLs.

2. RHPIC-LBM

Method, Algorithm, Code, Validation

RHPIC-LBM: Method & Algorithm & code & Validation

3D Hybrid Hypersingular Integral Equation(HHIE) 2002.09 ~ 2008.01

3D Hybrid Hypersingular Integral Equation-Lattice Boltzmann Method(HHIE-LBM) 2008.01 ~ 2013.01

3D Lattice Green Function-Lattice Boltzmann Method(LGM-LBM) Parallel CPU & GPU 2013.01 ~ 2015.07

Hybrid method combined the Particle-in-Cell (PIC) and Lattice Boltzmann Method (HPIC-LBM)
(2D/2.5D Kinetic-Dynamic-Hydro) 2015.07 ~ 2016.10

Relativistic HPIC-LBM
(2D/2.5D Kinetic-Dynamic-Hydro) 2016.10 ~ 2017.10

Validation 2017.10 ~ 2018.03

Developed and added new Program modules: Turbulence induced anomalous resistivity and viscosity
(3D Kinetic-Dynamic-Hydro) 2018.03 ~ 2021.07

Parallel CPU&GPU Version
(3D Kinetic-Dynamic-Hydro) 2021.07 ~ Now

US NSF Report: RHPIC-LBM Validation

Independent Intellectual Property Rights(IIPR)

1983 Sauro Succi, 2009 Andrew Declan Diver, 2015 Mohseni Farhang (Hans J Herrminer, Sauro succi,Bastien Chopard) , 2017 Wolf-Gladrow Dieter(Neubauer F.M, Lussem M) et.al, Zhu et al 2007,2013, 2019,2020a,2020b,2023a,2023b,2023c

PHPIC-LBM: Method

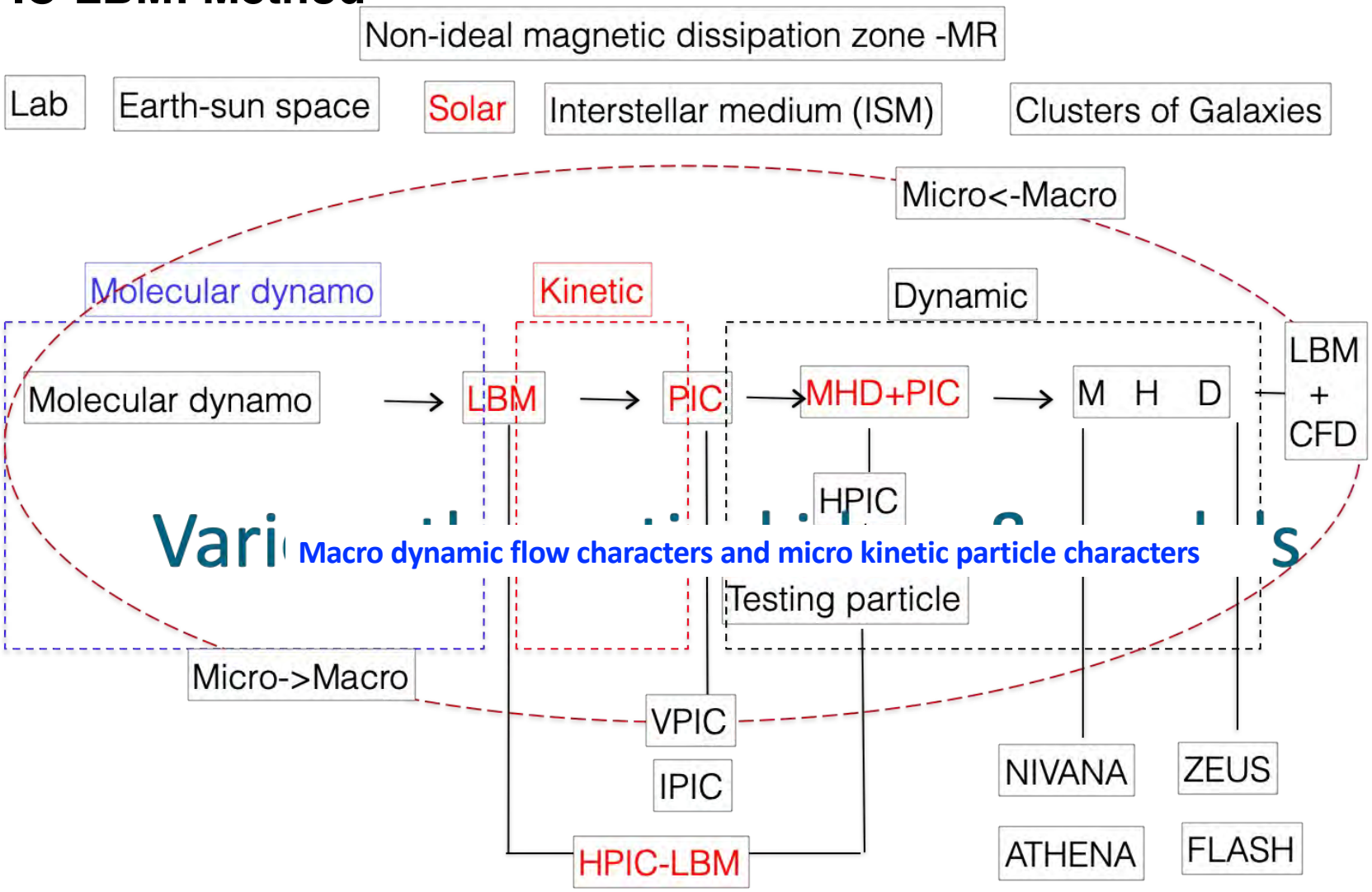

PHPIC-LBM: Method

$$\frac{\partial f_{\iota\xi\varrho}^{\varsigma e}}{\partial t}+\frac{1}{\varepsilon_\iota^e}\boldsymbol{U}_\iota^e\cdot\nabla_x f_{\iota\xi\varrho}^{\varsigma e}+\boldsymbol{F}_\iota^e\cdot\frac{\partial f_{\iota\xi\varrho}^{\varsigma e}}{\partial \boldsymbol{p}_\iota^e}=\frac{\theta_\iota^e}{(\varepsilon_\iota^e)^2}\nabla_{\boldsymbol{p}_\iota^e}\cdot\left(\nabla_{\boldsymbol{p}_\iota^e}f_{\iota\xi\varrho}^{\varsigma e}+\boldsymbol{U}_\iota^e f_{\iota\xi\varrho}^{\varsigma e}\right)\tag{8}$$

$$\frac{\partial f_{\iota\xi\varrho}^{\varsigma i}}{\partial t}+\frac{1}{\varepsilon_\iota^i}\boldsymbol{U}_\iota^i\cdot\nabla_x f_{\iota\xi\varrho}^{\varsigma i}+\boldsymbol{F}_\iota^i\cdot\frac{\partial f_{\iota\xi\varrho}^{\varsigma i}}{\partial \boldsymbol{p}_\iota^i}=\frac{\theta_\iota^i}{(\varepsilon_\iota^i)^2}\nabla_{\boldsymbol{p}_\iota^i}\cdot\left(\nabla_{\boldsymbol{p}_\iota^i}f_{\iota\xi\varrho}^{\varsigma i}+\boldsymbol{U}_\iota^i f_{\iota\xi\varrho}^{\varsigma i}\right)\tag{9}$$

$$\frac{\partial f_{\iota\xi\varrho}^{\varsigma n}}{\partial t}+\boldsymbol{U}_\iota^n\cdot\nabla_x f_{\iota\xi\varrho}^{\varsigma n}+\boldsymbol{F}_\iota^n\cdot\frac{\partial f_{\iota\xi\varrho}^{\varsigma n}}{\partial \boldsymbol{p}_\iota^n}=\nabla_{\boldsymbol{p}_\iota^n}\cdot\left(\nabla_{\boldsymbol{p}_\iota^n}f_{\iota\xi\varrho}^{\varsigma n}+\boldsymbol{U}_\iota^n f_{\iota\xi\varrho}^{\varsigma n}\right)\tag{10}$$

$$\frac{\partial\bar{\boldsymbol{B}}}{\partial t}=\nabla\times\left(\bar{\boldsymbol{U}}\times\bar{\boldsymbol{B}}\right)-\nabla\times\left(\hat{\alpha}\bar{\boldsymbol{B}}\right)+\hat{\beta}\nabla^2\bar{\boldsymbol{B}}+\mu^{-1}(\eta_s+\eta_{MT}+\eta_{FT})\nabla^2\bar{\boldsymbol{B}}\tag{11}$$

$$\frac{\partial\tilde{\boldsymbol{B}}}{\partial t}=\nabla\times\left(\bar{\boldsymbol{U}}\times\tilde{\boldsymbol{B}}\right)+\nabla\times\left(\tilde{\boldsymbol{U}}\times\bar{\boldsymbol{B}}\right)+\nabla\times\left(\tilde{\boldsymbol{U}}\times\tilde{\boldsymbol{B}}\right)-\nabla\times\left(\hat{\alpha}\bar{\boldsymbol{B}}\right)+\hat{\beta}\nabla^2\bar{\boldsymbol{B}}+\mu^{-1}(\eta_s+\eta_{MT}+\eta_{FT})\nabla^2\tilde{\boldsymbol{B}}\tag{12}$$

$$\frac{\partial\boldsymbol{B}}{\partial t}=\nabla\times\left\{\begin{array}{l}\underset{(a)}{\frac{m_e}{e}\frac{\partial\boldsymbol{U}_e}{\partial t}}+\underset{(b)}{\frac{m_e}{e}\left(\boldsymbol{U}_e\nabla\right)\boldsymbol{U}_e}+\underset{(c)}{\frac{1}{en_e}\nabla P_e}+\underset{(d)}{\frac{1}{en_e}\nabla\boldsymbol{\pi_e}}+\underset{(e)}{\frac{m_e}{e}\left\langle\xi\cdot\nabla\cdot\xi\right\rangle}+\underset{(f)}{\boldsymbol{U}_e\times\boldsymbol{B}}-\underset{(g)}{\alpha_\parallel\left(\boldsymbol{J}\cdot\boldsymbol{b}\right)\boldsymbol{b}}-\\ \underset{(h)}{\alpha_\perp\boldsymbol{b}\times\left(\boldsymbol{J}\times\boldsymbol{b}\right)}+\underset{(i)}{\alpha_\Lambda\left(\boldsymbol{b}\times\boldsymbol{J}\right)}+\underset{(j)}{\frac{\beta_\parallel}{e}\left(\nabla T_e\cdot\boldsymbol{b}\right)\boldsymbol{b}}+\underset{(k)}{\frac{\beta_\perp}{e}\boldsymbol{b}\times\left(\nabla T_e\times\boldsymbol{b}\right)}+\underset{(l)}{\frac{\beta_\Lambda}{e}\left(\boldsymbol{b}\times\nabla T_e\right)}+\underset{(m)}{\left\langle\xi\times\tilde{\boldsymbol{B}}\right\rangle}\end{array}\right\}\tag{13}$$

$$\frac{\partial f_{1\xi\varrho}^{\varsigma n}}{\partial t}+\frac{1}{\varepsilon_1^n}\boldsymbol{U}_1^n\cdot\nabla_x f_{1\xi\varrho}^{\varsigma n}+\boldsymbol{F}_1^n\cdot\frac{\partial f_{1\xi\varrho}^{\varsigma n}}{\partial \boldsymbol{p}_1^n}=\frac{\theta_1^n}{(\varepsilon_1^n)^2}\nabla_{\boldsymbol{p}_1^n}\cdot\left(\nabla_{\boldsymbol{p}_1^n}f_{1\xi\varrho}^{\varsigma n}+\boldsymbol{U}_1^n f_{1\xi\varrho}^{\varsigma n}\right)\tag{15}$$

$$\boldsymbol{F}_1^n=\nabla\cdot\left[\rho\boldsymbol{U_1}\boldsymbol{U_1}\boldsymbol{I}+p\boldsymbol{I}-\xi_n^{TVD}\nabla\cdot\boldsymbol{U}_1-\rho g\right]-\nabla\cdot\left\{(\vartheta_{n0}^{VD}+\xi_n^{TVD})\left[\nabla\boldsymbol{U_1}+(\nabla\boldsymbol{U_1})^\top-\frac{2\nabla\cdot\boldsymbol{U_1}}{3}I\right]\right\}\tag{16}$$

The Relativistic HPIC-LBM Code based on Plasma Statistical Physics Framework

PHPIC-LBM: Method

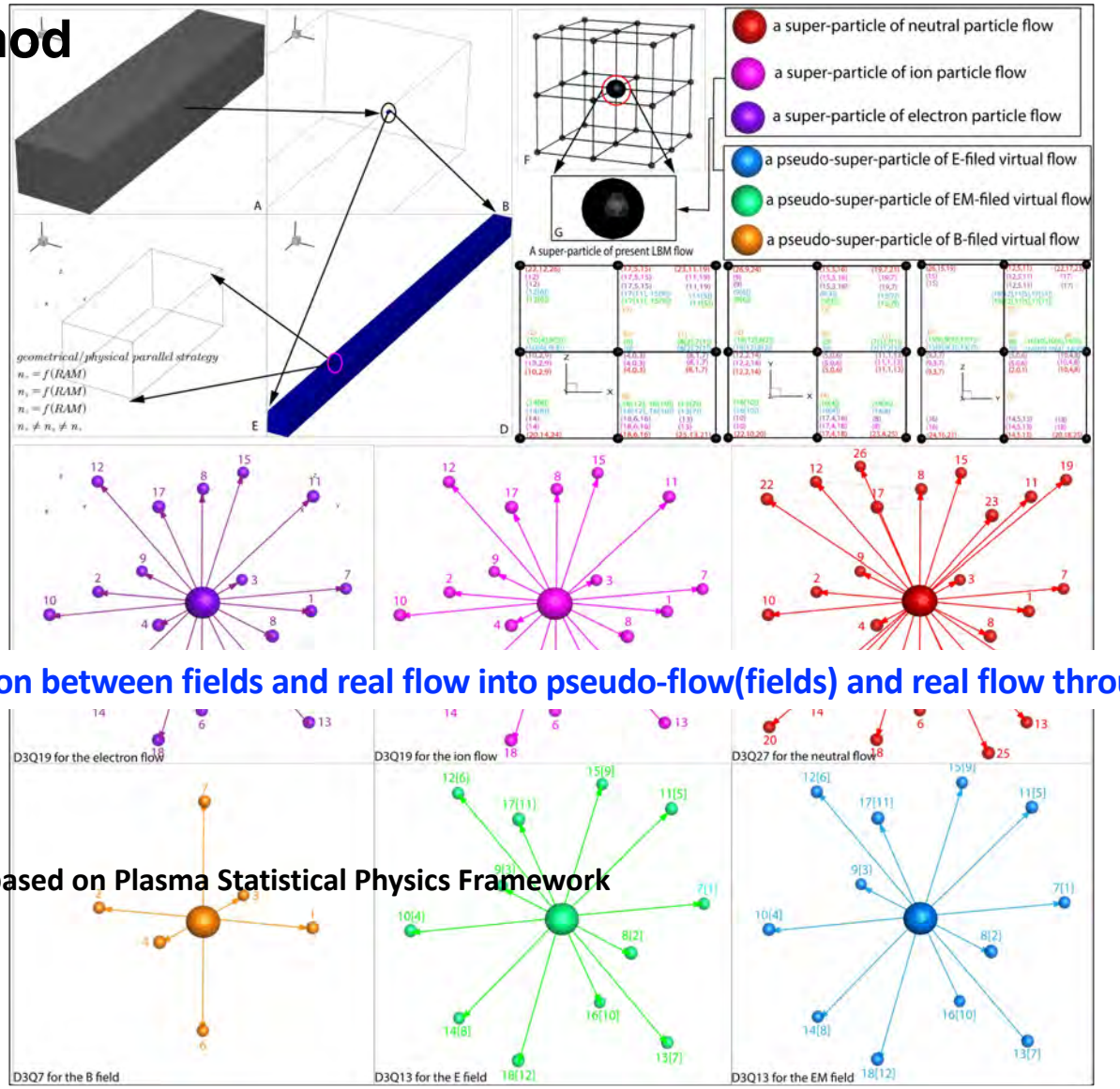

Convert the interaction between fields and real flow into pseudo-flow(fields) and real flow through lattice grid model

The Relativistic HPIC-LBM Code based on Plasma Statistical Physics Framework

RHPIC-LBM Method Turbulence induced viscosity & resistivity dissipation and diffusion model

Definition: eddy-viscosity type resistivity coefficient MHD magnetic dissipation region of LSTMR

$$\alpha = -\frac{1}{3}\int_{-\infty}^{t}\left\langle \tilde{\boldsymbol{V}}\cdot\nabla\times\tilde{\boldsymbol{V}}'\right\rangle dt' = -\frac{1}{3}\tau_\alpha\left\langle \tilde{\boldsymbol{V}}\cdot\nabla\times\tilde{\boldsymbol{V}}\right\rangle = -\frac{1}{3}\tau_\alpha \boldsymbol{H}^{\boldsymbol{K}} = -\frac{1}{3}\tau_\alpha\int_{Volume}(\boldsymbol{V}\cdot\nabla\times\boldsymbol{V})dx^3$$

$\boldsymbol{V}\cdot\nabla\times\boldsymbol{V}$ The helicity density $\boldsymbol{H}^{\boldsymbol{K}}$ The kinetic helicity

The mean component of velocity and magnetic field parts-----pseudo scaler-----B

$$\eta_t^M = \frac{1}{3}\int_{-\infty}^{t}\left\langle \tilde{\boldsymbol{V}}\cdot\tilde{\boldsymbol{V}}'\right\rangle dt' = \frac{1}{3}\tau_\beta\left\langle \tilde{\boldsymbol{V}}^2\right\rangle = \frac{1}{3}\tau_\beta \boldsymbol{E}^{\boldsymbol{K}}$$

$\boldsymbol{E}^{\boldsymbol{K}}$ The kinetic energy of turbulence

The fluctuatingcomponent of velocity and magnetic field parts-----pseudo scaler-----J

$\eta_t^V \sim \omega \qquad \omega = \nabla\times\boldsymbol{V}$

The fluctuatingcomponent of velocity and magnetic field parts-----pseudo scaler-----ω

Definition: Spitzer resistivity

$$\eta_s = \frac{\pi Z e^2 \ln\Lambda\sqrt{m_e}}{(4\pi\varepsilon_0)^2(K_B T_e)^{3/2}} = \frac{\eta c^2}{4\pi}$$

$$\eta_s|_\perp = 1.96\eta_s|_\parallel = 1.03\times10^{-4}T_-^{-3/2}Z\ln\Lambda \approx 1.03\times10^{-4}\ln\left(\frac{Z^{1.71828}T_e^{1.72313}}{\cdots}\right)$$

Viscous induced dissipation (VD, ϑ_{n0}, ξ_n^{PT}, ξ_n^{TT}, ϑ_{i0}, ξ_i^{PT}, ξ_i^{TT}, ϑ_{e0}, ξ_e^{PT}, ξ_e^{TT}, see Appendix B and

1^{st} type: Plasma bulk kinetic energy ($E_{\boldsymbol{U}}$) dissipation into plasma heating energy ($E_{\boldsymbol{T}}$) and non-thermal kinetic energy that accelerates particles ($E_{\boldsymbol{SEP}}$, here we will focus on the solar energetic particles, SEP)(e.g., Duijveman 1981; Ryan et al. 2000; Tandberg-Hanssen 2009; Antolin et al. 2020; Pontinet al. 2020);

2^{nd} type: $E_{\boldsymbol{U}}$ dissipation into magnetic energy ($E_{\boldsymbol{B}}$).

Definition: non-ideal MHD magnetic dissipation region of LSTMR

Mathematical model: assuming that magnetic dissipation effects depend mainly on **the current density** a Taypor expansion gives

$$\boldsymbol{E}+\boldsymbol{V}\times\boldsymbol{B} = \eta_1\boldsymbol{j} - \eta_2\nabla^2\boldsymbol{j} + \cdots\cdots \qquad \eta_1 = \left(\frac{c}{\omega_{pe}}\right)^2 \upsilon_e \qquad \eta_2 \simeq \left(\frac{c}{\omega_{pe}}\right)^2 \mu_e$$

υ_e Electron-ion collision frequency $\mu_e \sim r_e^2\upsilon_e$ Electron viscosity

$\omega_{pe} = e\sqrt{4\pi n/m_e}$ Electron plasma frequency

?

Physical model: Dividing the fields into mean and fluctuating parts, the mean turbulence energy-dissipation rate closed linked eddy-viscosity can be written as

$$\varepsilon = \alpha\langle\boldsymbol{B}\rangle - \eta_t^M\langle j\rangle + \eta_t^V\langle\omega\rangle = \alpha_t\langle\boldsymbol{B}\rangle - \eta_t^M\langle\nabla\times\boldsymbol{B}\rangle + \eta_t^V\langle\nabla\times\boldsymbol{V}\rangle$$

Physical model: split the velocity and magnetic field into mean and fluctuating parts, from mean field kinematic dynamo theory, the induction equation can be written as

$$\frac{\partial\boldsymbol{B}}{\partial t} = \nabla\times(\boldsymbol{V}\times\boldsymbol{B}) + \nabla\times\left(\tilde{\boldsymbol{V}}\times\tilde{\boldsymbol{B}}\right) + \eta_s\nabla^2\tilde{\boldsymbol{B}}$$

Resistive induced dissipation (RD, $\eta_n^{\circlearrowleft}$, $\eta_n^{\prime}$, $\eta_i^{\prime}$, $\eta_e^{\prime}$, see Appendix B and following sections 2.1 for def-

According to the classification criteria of resistivity properties of solar plasma, the energy dissipation in this process can be categorized into two different categories depending on the coherent structures of $\boldsymbol{B}$-turbulence:

3^{rd} type: $E_{\boldsymbol{B}}$ dissipation into $E_{\boldsymbol{T}}$ and $E_{\boldsymbol{SEP}}$;

4^{th} type: $E_{\boldsymbol{B}}$ dissipation into $E_{\boldsymbol{U}}$.

Resistivity and Viscosity

RHPIC-LBM Method Turbulence induced viscosity & resistivity dissipation and diffusion model

CLS	L_{LE}	$L^M_{U_A}$	$L^{PT}_{\xi_n}$	$L^{TT}_{\xi_n}$	$L^S_{\eta_n}$	$L^T_{\eta_n}$	L_i	$L^{PT}_{\xi_i}$	$L^{TT}_{\xi_i}$	$L^T_{\eta_i}$	$L^K_{U_A}$	L_e	$L^{PT}_{\xi_e}$	$L^{TT}_{\xi_e}$	$L^T_{\eta_e}$
I(1-3): ($l > L_{\xi_n}{}^{PT}$), FC, LEM, KLS															
I(1): Electric neutral fluid ($l > L_{LE} >> L^M_{U_A}$)															
I(2): Ideal electrically conducting MHD ($L_{LE} > l > L^M_{U_A}$),															
I(3): Quasi-neutral ideal MHD($L^M_{U_A} > L > L_{\xi_n}{}^{PT}$)															
$EC_{dyn}\|_{HD}$	(✓[a])	$I(1)\times$[b], $I(2)$✓	×	×	×	×	×	×	×	×	×	×	×	×	×
$EC_{dyn}\|_{MHD}$	×	$I(3)$✓	×	×	×	×	×	×	×	×	×	×	×	×	×
II(1-2): ($L^{PT}_{\xi_n} > l > L^S_{\eta_n}$), FC															
II(1): Quasi-neutral non-ideal MHD ($L^{PT}_{\xi_n} > L > L^{TT}_{\xi_n}$), KLS, VD/TVD [$\xi_n{}^{PT}$]															
II(2): WIP non-ideal MHD($L^{TT}_{\xi_n} > L > L^S_{\eta_n}$), TAC, VD/TVD [$\xi_n{}^{PT}$,$\xi_n{}^{TT}$]															
$VD_\vartheta\|_{HD}$	×	×	✓	✓	✓	✓	×	×	×	×	×	×	×	×	×
$VD_\xi\|_{HD}$	×	×	×	✓	✓	✓	×	×	×	×	×	×	×	×	×
III(1-3): ($L^S_{\eta_n} > l > L_{\xi_i}{}^{PT}$), TAC															
III(1): WIP non-ideal MHD to PIP non-ideal MHD ($L^S_{\eta_n} > L > L^T_{\eta_n}$), FC, VD/TVD [$\xi_n{}^{PT}$], RD/TRD [$\eta_n^S$]															
III(2): PIP non-ideal MHD($L^T_{\eta_n} > L > L_i$), FC&PC, VD/TVD [$\xi_n{}^{PT}$, $\xi_n{}^{TT}$], RD/TRD [η_n^S, η_n^T]															
III(3): FIP MHD ($L_i > l > L_{\xi_i}{}^{PT}$), FC&PC, VD/TVD [$\xi_n{}^{PT}$, $\xi_n{}^{TT}$], RD/TRD [η_n^S, η_n^T],HMHD [L_i]															
$VD_\xi\|_{MHD}$	×	×	×	×	✓	✓	✓	✓	×	×	×	×	×	×	×
$RD_{\eta_s}\|_{MHD}$	×	×	×	×	✓	✓	×	×	×	×	×	×	×	×	×
$RD_{\eta^T}\|_{MHD}$	×	×	×	×	×	✓	×	×	×	×	×	×	×	×	×
$HMDD$	×	×	×	×	✓	✓	✓	✓	✓	✓	✓	✓	✓	✓	✓
IV(1-2): ($L^{PT}_{\xi_i} > l > L_{\eta i}{}^T$), FIP MHD, FC&PC,TAC															
IV(1): ($L^{PT}_{\xi_i} > l > L^{TT}_{\xi_i}$), VD/TVD [$\xi_n{}^{PT}$, $\xi_n{}^{TT}$, $\xi_i{}^{PT}$], RD/TRD [η_n^S, η_n^T]															
IV(2): ($L^{TT}_{\xi_i} > l > L^T_{\eta_i}$), VD/TVD [$\xi_n{}^{PT}$, $\xi_n{}^{TT}$, $\xi_i{}^{PT}$], RD/TRD [η_n^S, η_n^T, η_i^T]															
$VD_\vartheta\|_{IMHD}$	×	×	×	×	×	×	×	✓	✓	✓	✓	×	×	×	×
$VD_\xi\|_{IMHD}$	×	×	×	×	×	×	×	×	✓	✓	✓	×	×	×	×
$RD_{\eta^T}\|_{IMHD}$	×	×	×	×	×	×	×	×	✓	✓	✓	×	×	×	×
V(1-3): ($L^T_{\eta_i} > l > L^{PT}_{\xi_e}$), FIP MHD, FC&PC, TAC															
V(1): ($L^T_{\eta_i} > l > L^K_{U_A}$), FIP MHD, FC&PC, VD/TVD [$\xi_n{}^{PT}$, $\xi_n{}^{TT}$, $\xi_i{}^{PT}$, $\xi_i{}^{TT}$], RD/TRD [η_n^S, η_n^T, η_i^T], TAC															
V(2): ($L^K_{U_A} > l > L_e$) FIP MHD, FC&PC, VD/TVD [$\xi_n{}^{PT}$, $\xi_n{}^{TT}$, $\xi_i{}^{PT}$, $\xi_i{}^{TT}$], RD/TRD [η_n^S, η_n^T, η_i^T], TAC															
V(3): ($L_e > l > L^{PT}_{\xi_e}$) EMHD, FC&PC, VD/TVD [$\xi_n{}^{PT}$, $\xi_n{}^{TT}$, $\xi_i{}^{PT}$, $\xi_i{}^{TT}$], RD/TRD [η_n^S, η_n^T, η_i^T], TAC, MF															
$VD_\xi\|_{IMHD}$	×	×	×	×	×	×	×	✓	✓	✓	✓	×	×	×	
$RD^T_{\eta_i}\|_{IMHD}$	×	×	×	×	×	×	×	×	×	✓	✓	×	×	×	×
VI(1-2): ($L^{PT}_{\xi_e} > l > L_{\eta e}{}^T$), FIP MHD, FC&PC,TAC															
VI(1): ($L^{PT}_{\xi_e} > l > L^{TT}_{\xi_e}$) EMHD, VD/TVD [$\xi_n{}^{PT}$, $\xi_n{}^{TT}$, $\xi_i{}^{PT}$, $\xi_i{}^{TT}$, $\xi_e{}^{PT}$], RD/TRD [η_n^S, η_n^T, η_i^T]															
VI(2): ($L^{TT}_{\xi_e} > l > L^T_{\eta_e}$) EMHD, VD/TVD [$\xi_n{}^{PT}$, $\xi_n{}^{TT}$, $\xi_i{}^{PT}$, $\xi_i{}^{TT}$, $\xi_e{}^{PT}$, $\xi_e{}^{TT}$], RD/TRD [η_n^S, η_n^T, η_i^T]															
$VD_\vartheta\|_{EMHD}$	×	×	×	×	×	×	×	×	×	×	×	×	✓	✓	✓
$VD_\xi\|_{EMHD}$	×	×	×	×	×	×	×	×	×	×	×	×	×	✓	✓
$RD^T_\eta\|_{EMHD}$	×	×	×	×	×	×	×	×	×	✓	✓	×	×	×	×
VII ($L^T_{\eta_e} > l$) EMHD, FC&PC, VD/TVD [$\xi_n{}^{PT}$, $\xi_n{}^{TT}$, $\xi_i{}^{PT}$, $\xi_i{}^{TT}$, $\xi_e{}^{PT}$, $\xi_e{}^{TT}$], RD/TRD[η_n^S, η_n^T, η_i^T, η_i^T], TAC															
$RD^T_{\eta_e}\|_{EMHD}$	×	×	×	×	×	×	×	×	×	×	×	×	×	×	✓

[a] ✓: Energy dissipation (e.g., EC, VD/TVD, RD/TRD, Hall effect dissipation, and so on) happen at this special CLS.

[b] ×: Energy dissipation (e.g., EC, VD/TVD, RD/TRD, Hall effect dissipation, and so on) don't happen at this special CLS.

NOTE—For symbol definitions, see Appendix B.

Table 4. GR and PPC under different scales

ϱ	ξ	Hurst index, H_ϱ	GR (cm)	PPC[a]	Space Unit (cm)	Time Unit (s)	Frequency Unit (rad.s^{-1})
1	1	H_1	$c\omega_{pi}^{-1} \sim 9\times10^3$	$\mathcal{Z}^{\hat{n}(H_1)}$	$c\omega_{pi}^{-1} \sim 9\times10^3$	$1000\omega_{pi}^{-1} \sim 3.2\times10^{-3}$	×[b]
2 ~ 3	3	H_2[c], H_3[d]	$c\omega_{pi}^{-1} \sim 9\times10^3$	$\mathcal{Z}^{\hat{n}(H_2)}$, $\mathcal{Z}^{\hat{n}(H_3)}$[d]	$c\omega_{pi}^{-1} \sim 9\times10^3$	$\omega_{pi}^{-1} \sim 3.2\times10^{-7}$	$\omega_{pi} \sim 3.1\times10^6$
4	2	H_4	$c\omega_{pi}^{-1} \sim 9\times10^3$	$\mathcal{Z}^{\hat{n}(H_4)}$	$c\omega_{pi}^{-1} \sim 9\times10^3$	$\omega_{pi}^{-1} \sim 3.2\times10^{-7}$	$\omega_{pi} \sim 3.1\times10^6$
5	2	H_5	$c\omega_{pi}^{-1} \sim 9\times10^3$	$\mathcal{Z}^{\hat{n}(H_5)}$	$c\omega_{pi}^{-1} \sim 9\times10^3$	$\omega_{pi}^{-1} \sim 3.2\times10^{-7}$	$\omega_{pi} \sim 3.1\times10^6$
6	2	H_6	$c\omega_{pe}^{-1} \sim 5$[e]	$\mathcal{Z}^{\hat{n}(H_6)}$	$c\omega_{pe}^{-1} \sim 5$	$\omega_{pe}^{-1} \sim 0.17\times10^{-9}$	$\omega_{pe} \sim 5.64\times10^9$

[a] The Hurst index determined the PPC.

[b] ×: No frequency Unit at this scale.

[c] For neutrals fluid flow.

[d] For electron fluid flow and ion fluid flow.

[e] Same order with electron Debye Length inside the current sheet,λ_{De} (e.g., Narita et al. 2020; Maiorano et al. 2020; Settion 2020).

NOTE—For symbol definitions, see Appendix B.

Table 5. Non-dimensional viscosity and resistivity under different scales

ϱ	ξ	ϑ_{n0}	ϑ_n^{PT}	ξ_n^{TT}	ϑ_{i0}	ϑ_i^{PT}	ξ_i^{TT}	ϑ_{e0}	ϑ_e^{PT}	ϑ_e^{TT}	η_n^S	η_n^T	η_i^T	η_e^T
1	1	$\times10^{-4}$	$\frac{C_1E^2_{U_n}}{\epsilon_{U_n}}$	$\frac{C_2E^2_{U_n}}{\epsilon_{U_n}}$	×[a]	×	×	×	×	×	×	×	×	×
2,3	3	$\times10^{-4}$	$\frac{C_1E^2_{U_n}}{\epsilon_{U_n}}$	$\frac{C_2E^2_{U_n}}{\epsilon_{U_n}}$	$\frac{m_i(\kappa T_i)^{\frac{5}{2}}}{C_3e^4\ln\Lambda}$	$\frac{C_1E^2_{U_i}}{\epsilon_{U_i}}$	$\frac{C_2E^2_{U_i}}{\epsilon_{U_i}}$	$\frac{m_e(\kappa T_e)^{\frac{5}{2}}}{C_3e^4\ln\Lambda}$	$\frac{C_2E^2_{U_i}}{\epsilon_{U_i}}$	$\frac{C_2E^2_{U_i}}{\epsilon_{U_i}}$	η^S_{ni}[b], η^S_{ne}[c]	$\frac{1}{4\pi\sigma_T^i}$[d]	$\frac{1}{4\pi\sigma_T^i}$[e]	$\frac{1}{4\pi\sigma_T^e}$[f]
4	2	×	×	×	$\frac{m_i(\kappa T_i)^{\frac{5}{2}}}{C_3e^4\ln\Lambda}$	1	1	$\frac{m_e(\kappa T_e)^{\frac{5}{2}}}{C_3e^4\ln\Lambda}$	1	1	η^S_{ni}, η^S_{ne}	×	$\frac{1}{4\pi\sigma_T^i}$	$\frac{1}{4\pi\sigma_T^e}$
5	2	×	×	×	$\frac{m_i(\kappa T_i)^{\frac{5}{2}}}{C_3e^4\ln\Lambda}$	1	1	$\frac{m_e(\kappa T_e)^{\frac{5}{2}}}{C_3e^4\ln\Lambda}$	1	1	η^S_{ni}, η^S_{ne}	×	$\frac{1}{4\pi\sigma_T^i}$	$\frac{1}{4\pi\sigma_T^e}$
6	2	×	×	×	$\frac{m_i(\kappa T_i)^{\frac{5}{2}}}{C_3e^4\ln\Lambda}$	1	1	$\frac{m_e(\kappa T_e)^{\frac{5}{2}}}{C_3e^4\ln\Lambda}$	1	1	η^S_{ni}, η^S_{ne}	×	$\frac{1}{4\pi\sigma_T^i}$	$\frac{1}{4\pi\sigma_T^e}$

[a] The PPC is determined by the Hurst index.

[b] $\eta^S_{ni} = \eta_0 + \eta_1 \frac{|J\times B||U_i|^2}{|B|^2}$, $\eta_0 = 5.0\times10^{-4}$, $\eta_1 = 1.0\times10^{-3}$(e.g., Piddington 1981; Barghouty et al. 1996; Brandenburg et al. 2008; Hazra et al. 2018; Dikpati et al. 2007; Mark et al. 2014; Inoue et al. 2014; ?; Bamba et al. 2020; Miyoshi et al. 2020; Kusano et al. 2020).

[c] $\eta^S_{ne} = \eta_0 + \eta_1 \frac{|J\times B||U_e|^2}{|B|^2}$.

[d] $\sigma_T = \frac{\sqrt{3}c\sigma}{\sqrt{3c^2+4\pi UL_\varrho}}$, $U = \frac{U_n+U_i+U_e}{3}$

[e] $\sigma_T^i = \frac{\sqrt{3}c\sigma}{\sqrt{3c^2+4\pi U_iL_\varrho}}$

[f] $\sigma_T^e = \frac{\sqrt{3}c\sigma}{\sqrt{3c^2+4\pi U_eL_\varrho}}$

[g] $ln\Lambda = ln\frac{2}{2e^3}\begin{cases}\left(\frac{\kappa^3T_e^3}{\pi n_e}\right)^{1/2} & T_e < 5.8\times10^5\\ 100\times\left(\frac{58\kappa^3T_e^2}{\pi n_e}\right)^{1/2} & T_e > 5.8\times10^5\end{cases}$ (e.g., Chapman 1953; Leontovich 1967; Somov 1991, 2008, 2013; Gordovskyy 2020; Muhamad 2020)

NOTE—For symbol definitions, see Appendix B.

RHPIC-LBM Method

Multi-component-abundance-isotope model

Table 1. Chemical composition of the Sun

Chemical composition	Percent of the overall mass	Type
Hydrogen	**73%**	**Dominated**
Helium	25%	Dominated
Oxygen	0.8%	Metals
Carbon	0.36%	Metals
Iron	0.16%	Metals
Neon	0.12%	Metals
Nitrogen	0.09%	Metals
Silicon	0.07%	Metals
Magnesium	0.05%	Metals
Sulphur	0.04%	Metals
Others combined	0.04%	Metals

Electron, Proton, 3He， 4He with real proton-to-electron mass ratio & neutron-electron mass ratio

Table 2. Layers of the Sun

Layers	Thickness (km)	Temperature (K)	Type
Core	150, 000	10, 000, 000	Inertial layer
Convection Zone	180, 000	500, 000	Inertial layer
Photosphere[1]	400	6400	Outer layer, un-magnetized, weakly ionized
Chromosphere	2100	4400 – 8000	Outer layer, magnetized, partly ionized [2]
Transition region	100	8000 – 500, 000	Outer layer, magnetized, high ionized
Corona	5, 000, 000	1, 000, 000	Outer layer, magnetized, fully ionized

Multi-species & Multi-Degree of Ionization

RHPIC-LBM Algorithm

- Few things we need to know before running codes

(OpenCL，计算⑧、OpenGL，可视化⑩)

程序框架图

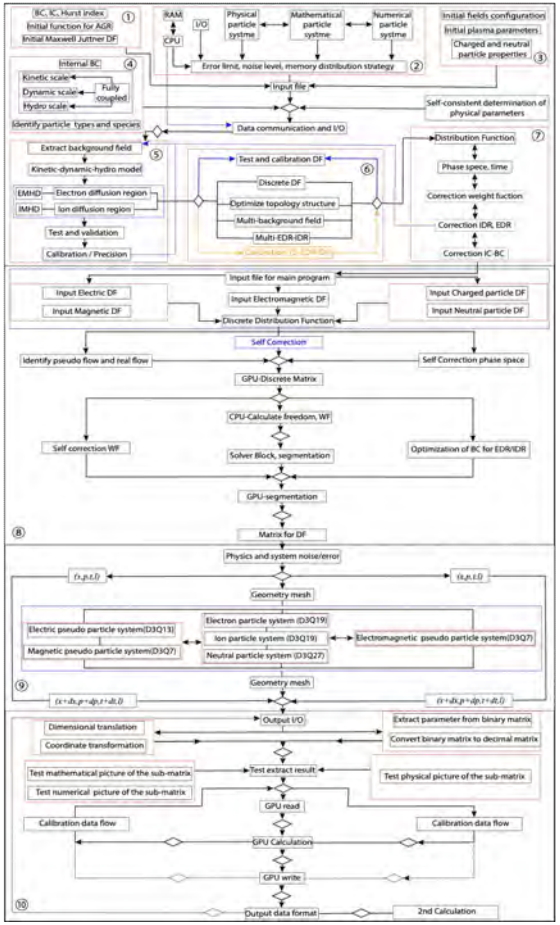

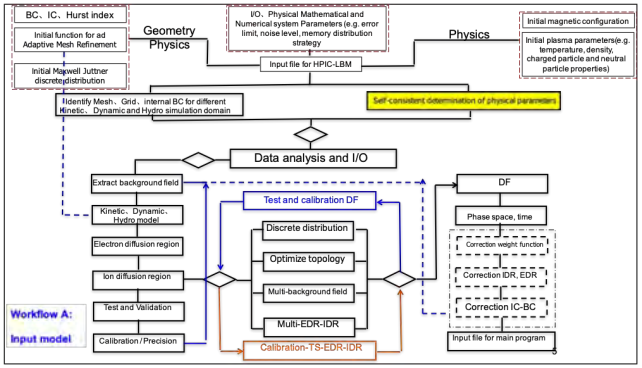

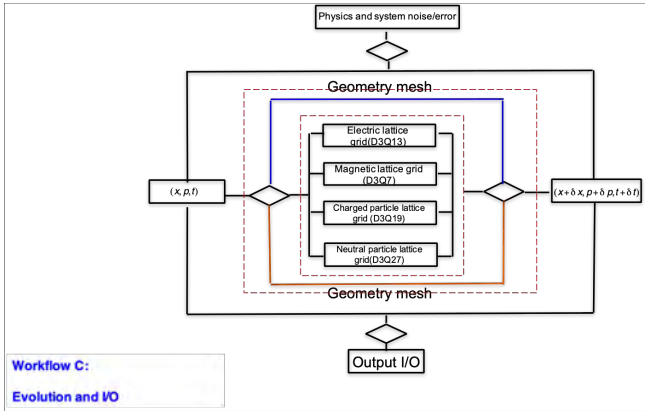

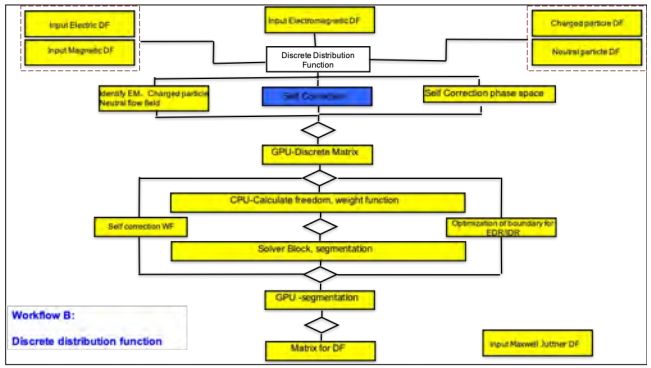

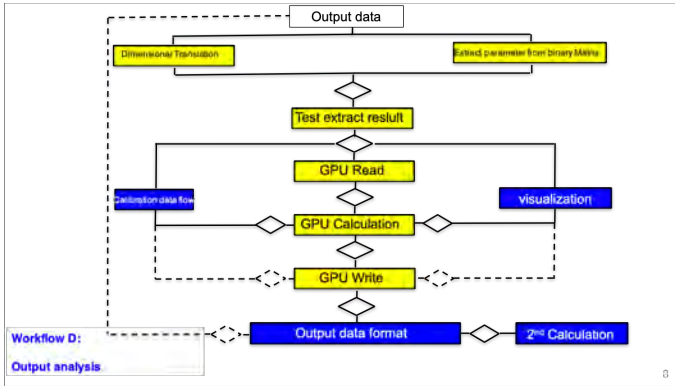

RHPIC-LBM code

伪代码图

- Few things we need to know before running codes

(OpenCL，计算⑧、OpenGL, 可视化⑩)

RHPIC-LBM code

X86 CPU Version (2014~2018)

CPU TIANHE-2(NUDT&NSCC-GZ) 2014 ~

CPU-DCU (2019-2023.7)

SUGON Heterogeneous DCU(NSCC-CAS) 2019 ~

CPU-GPU Version

ARM CPU (2023~)

ARM CPU TIANHE-3(NUDT&NSCC-TJ) 2023 ~

RHPIC-LBM validation

2.5D turbulence acceleration model I

Hybrid Acceleration Diffusive shock acceleration (DSA, 1st Fermi) & Stochastic acceleration(2nd Fermi)

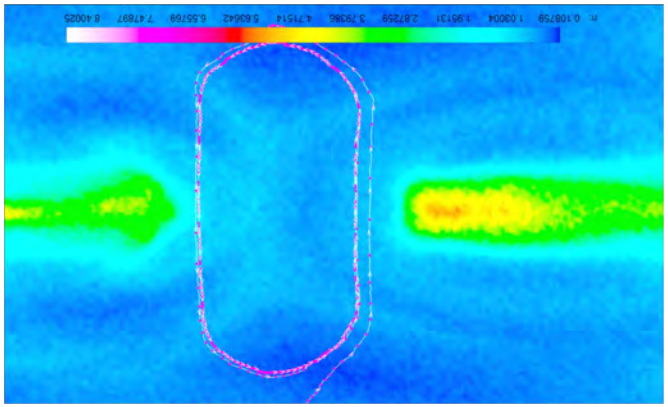

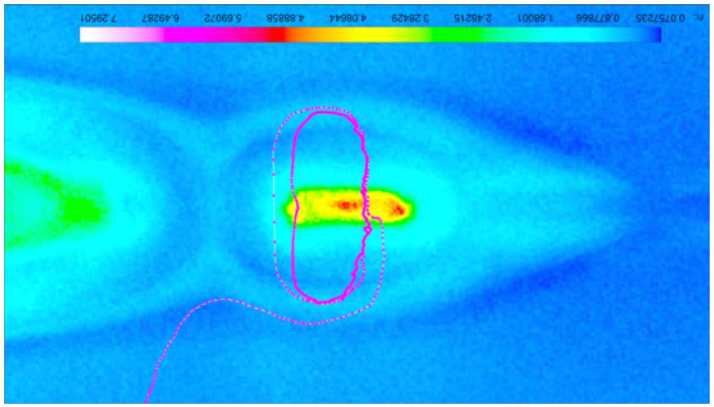

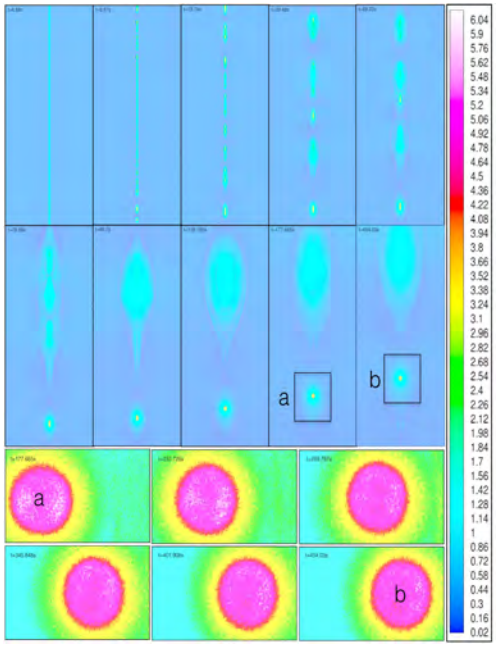

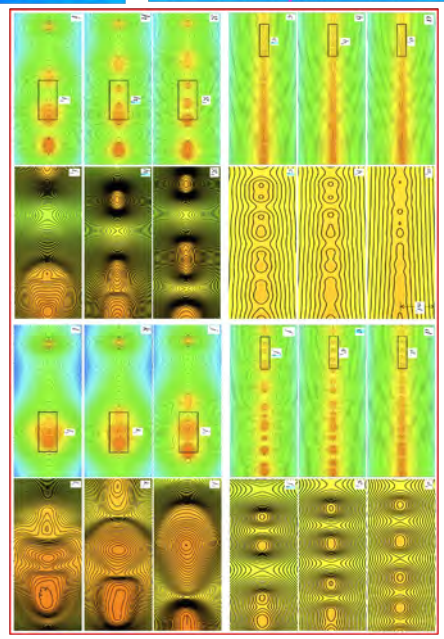

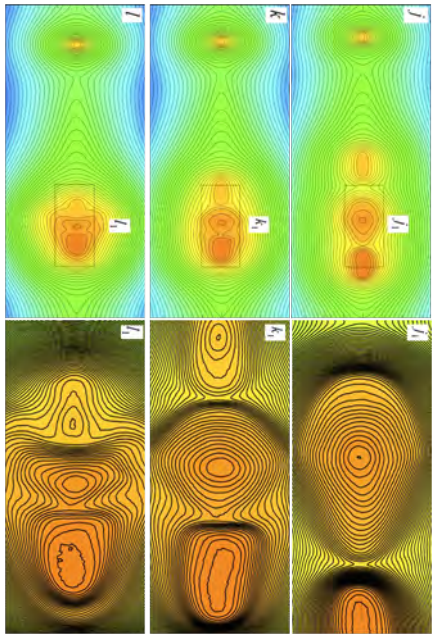

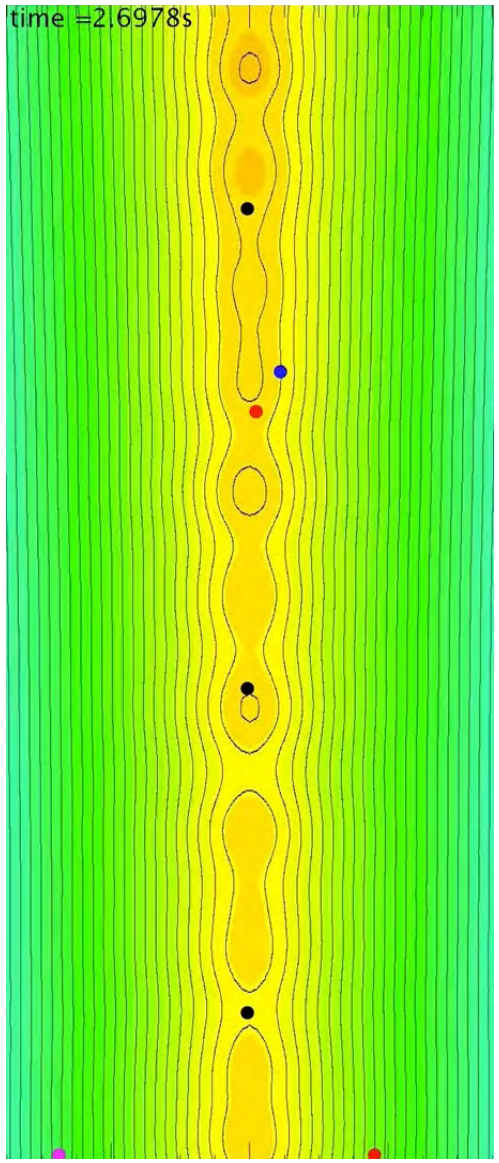

RHPIC-LBM validation

2.5D turbulence acceleration model I

Hybrid Acceleration Diffusive shock acceleration (DSA, 1st Fermi) & Stochastic acceleration(2nd Fermi)

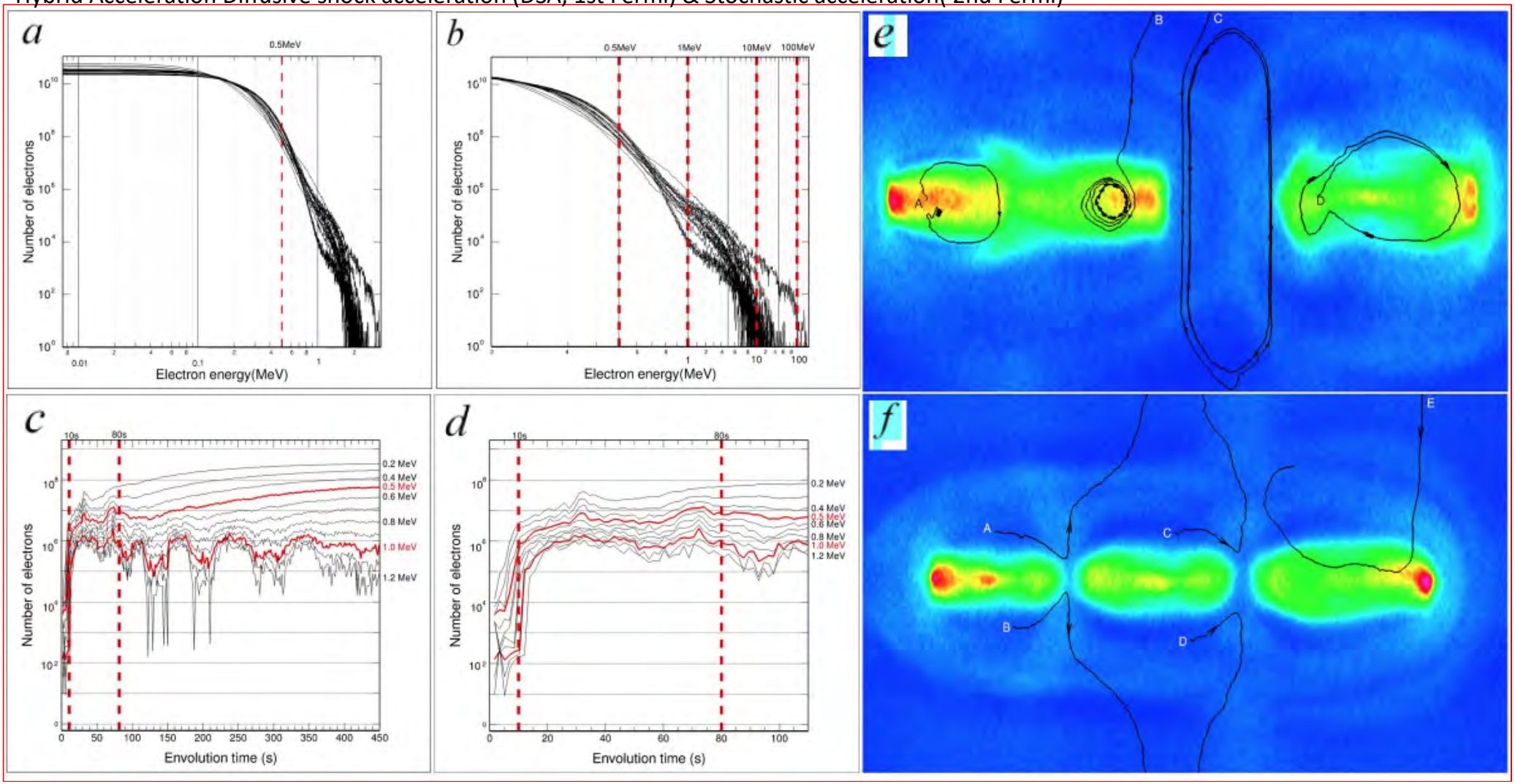

RHPIC-LBM validation 2.5D turbulence acceleration model II-Fractal CS

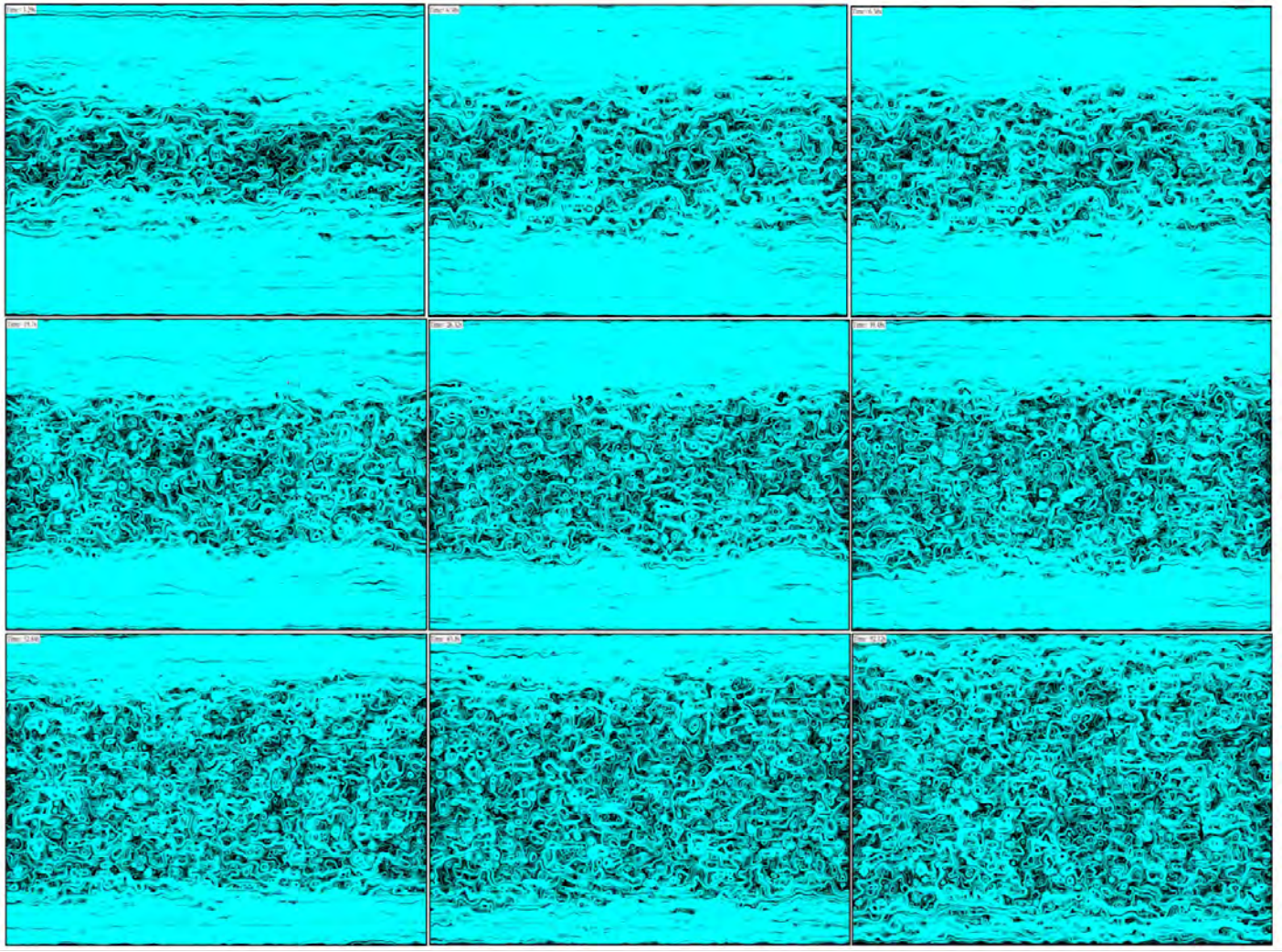

URL：https://pan.baidu.com/s/1ALXiDA4hEZhEES93p4o9nQ

RHPIC-LBM validation 2.5D turbulence acceleration model II-Fractal CS

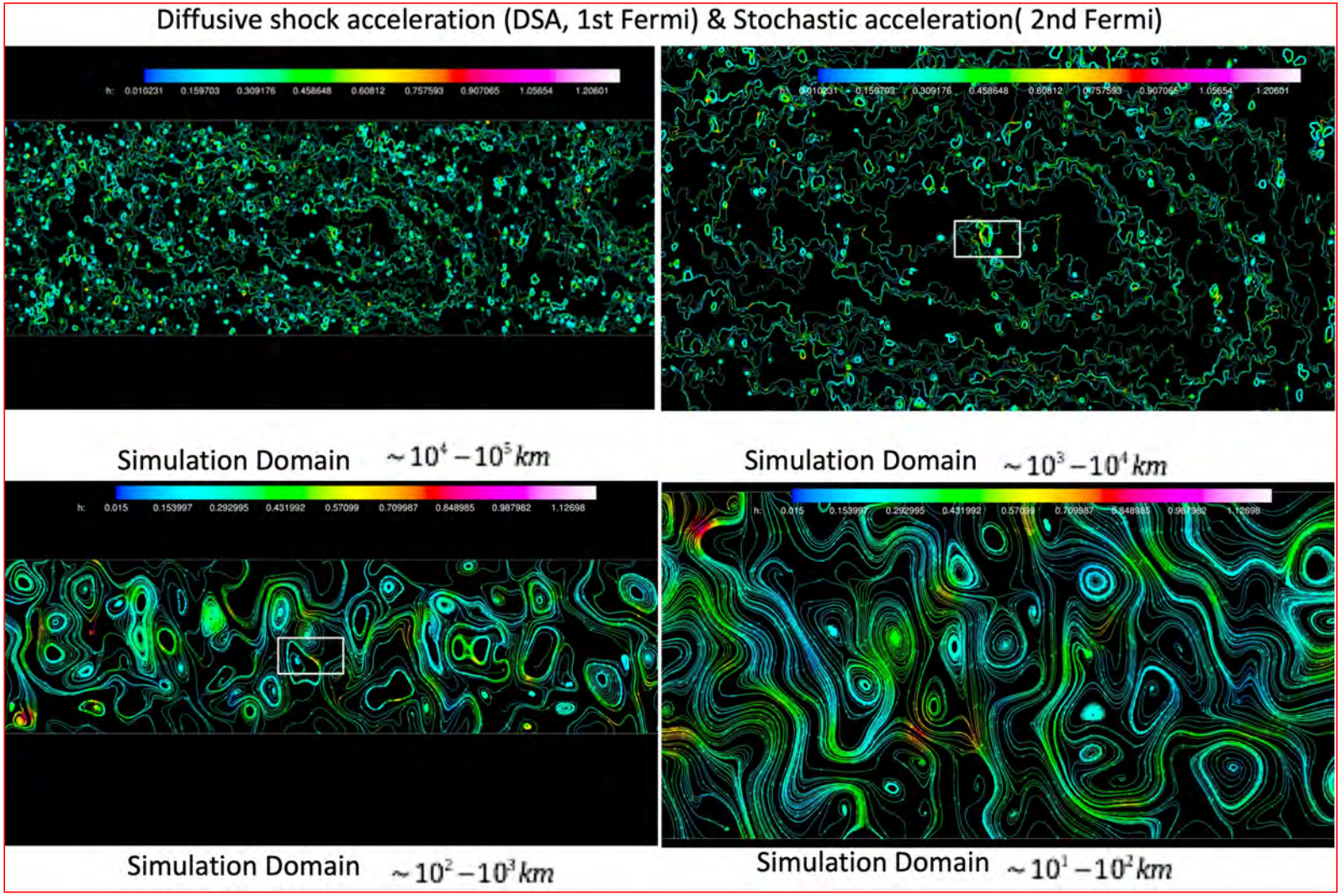

RHPIC-LBM validation 2.5D turbulence acceleration model II-Fractal CS

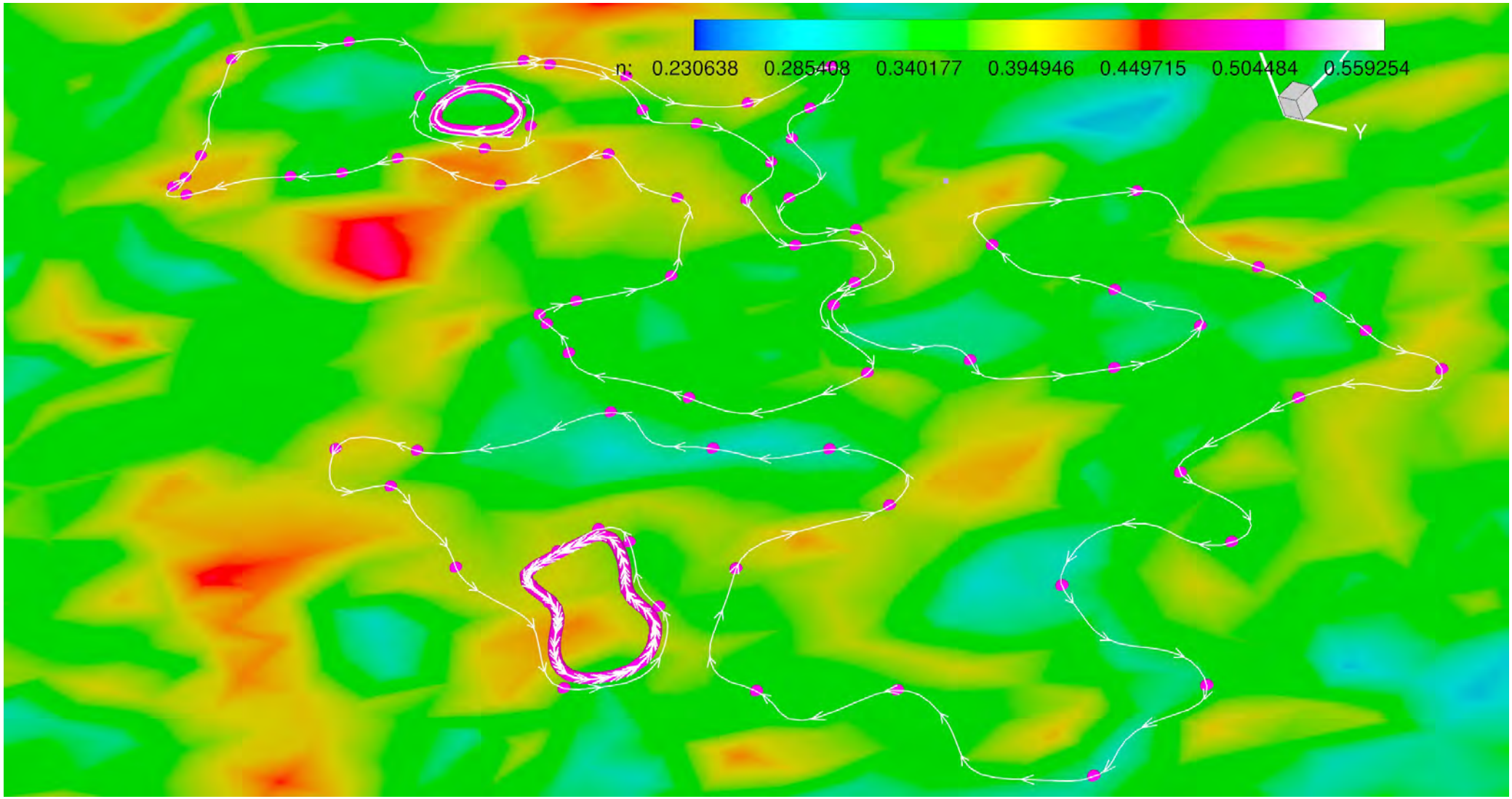

RHPIC-LBM validation

3D turbulence acceleration model I

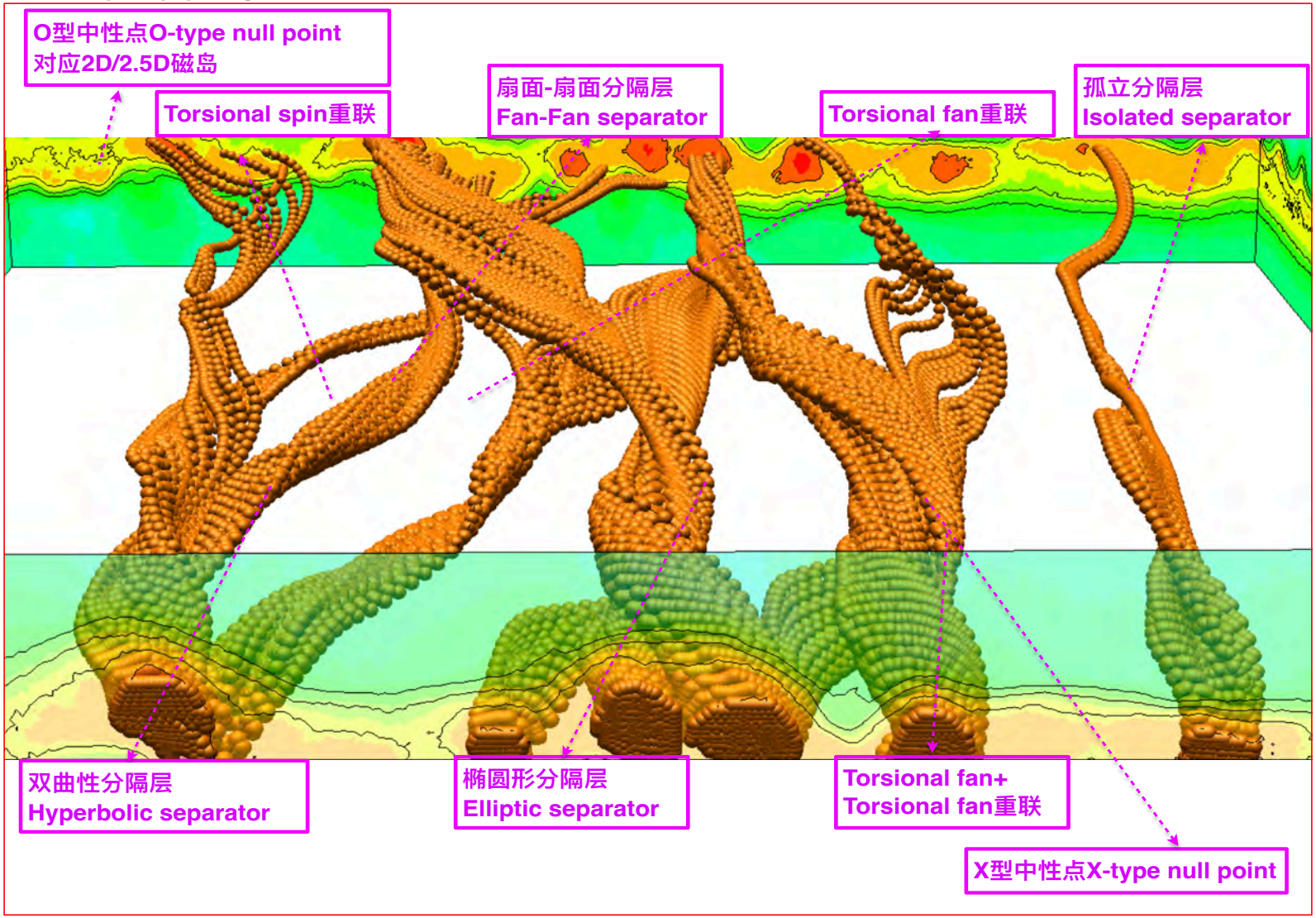

RHPIC-LBM validation

3D turbulence acceleration model I

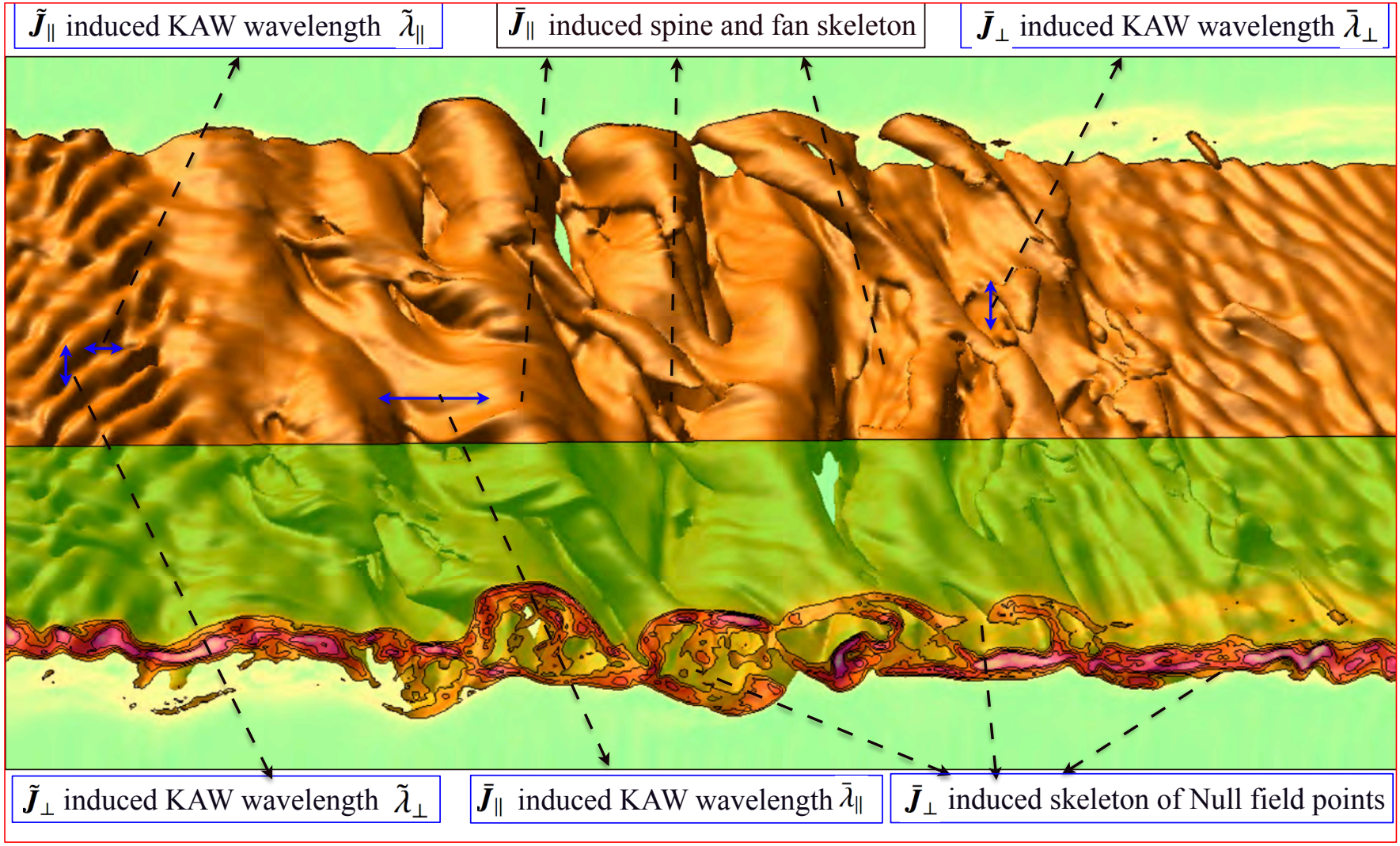

RHPIC-LBM validation

3D turbulence acceleration model I

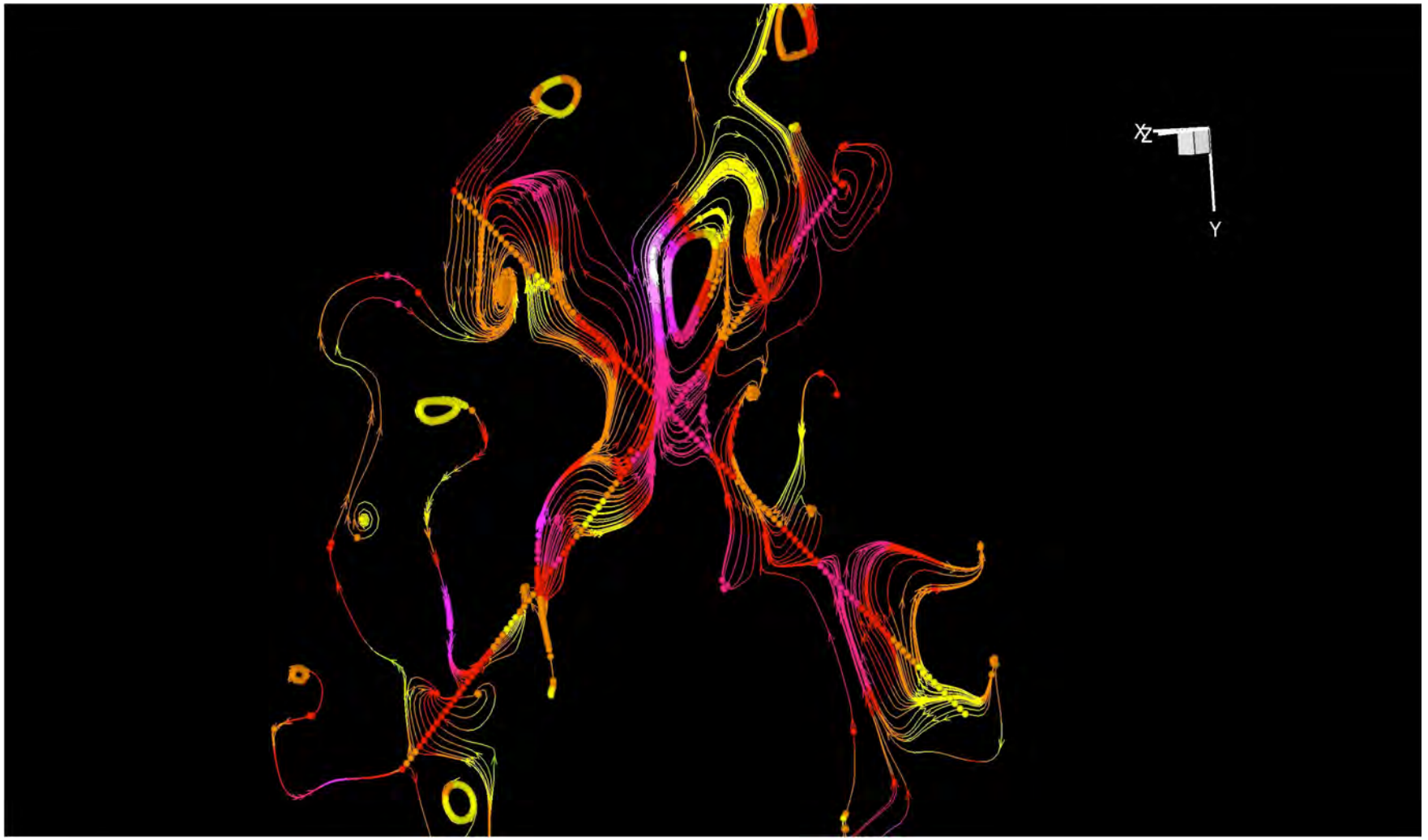

RHPIC-LBM validation

3D turbulence acceleration model I

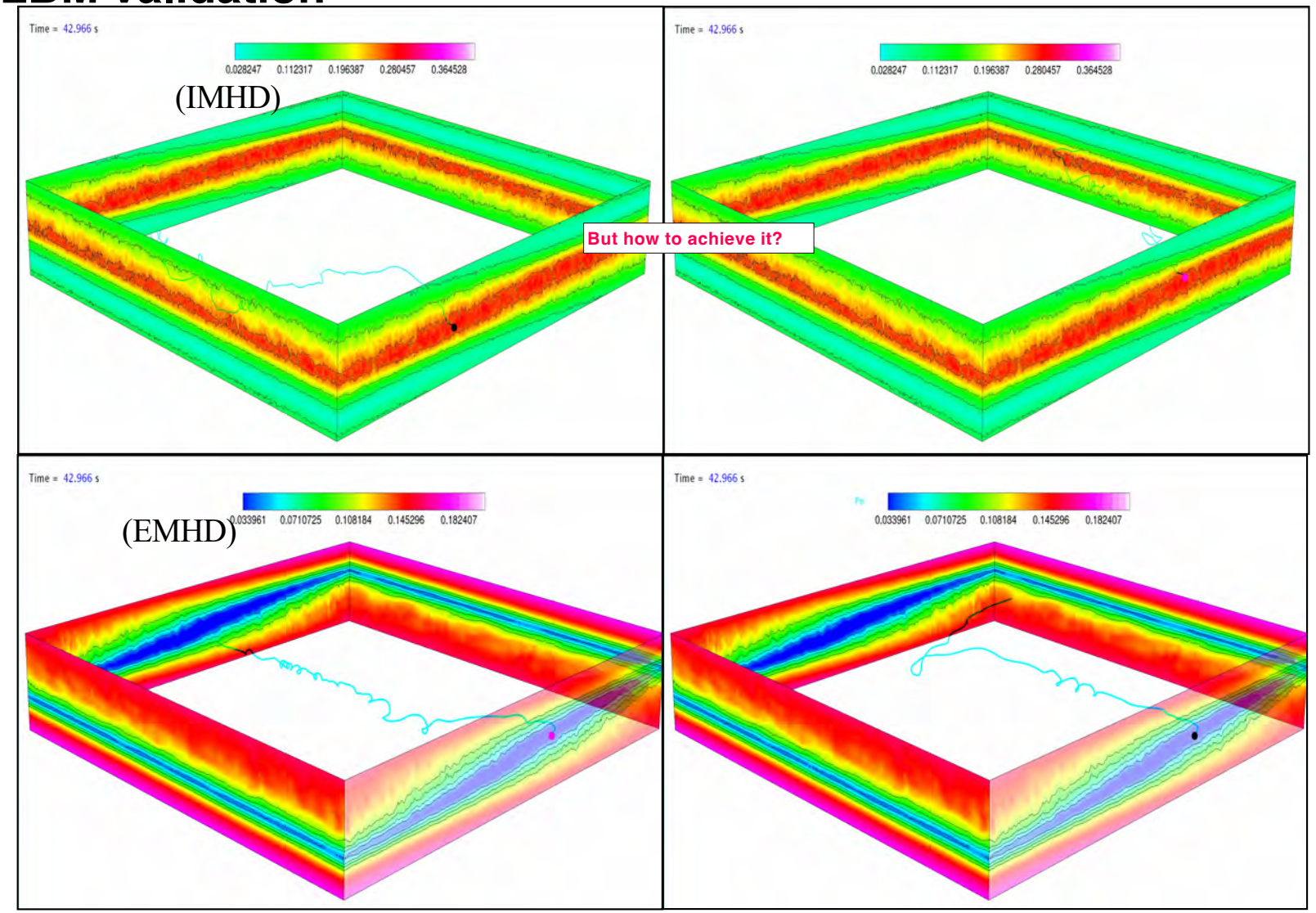

RHPIC-LBM validation

3D turbulence acceleration model I

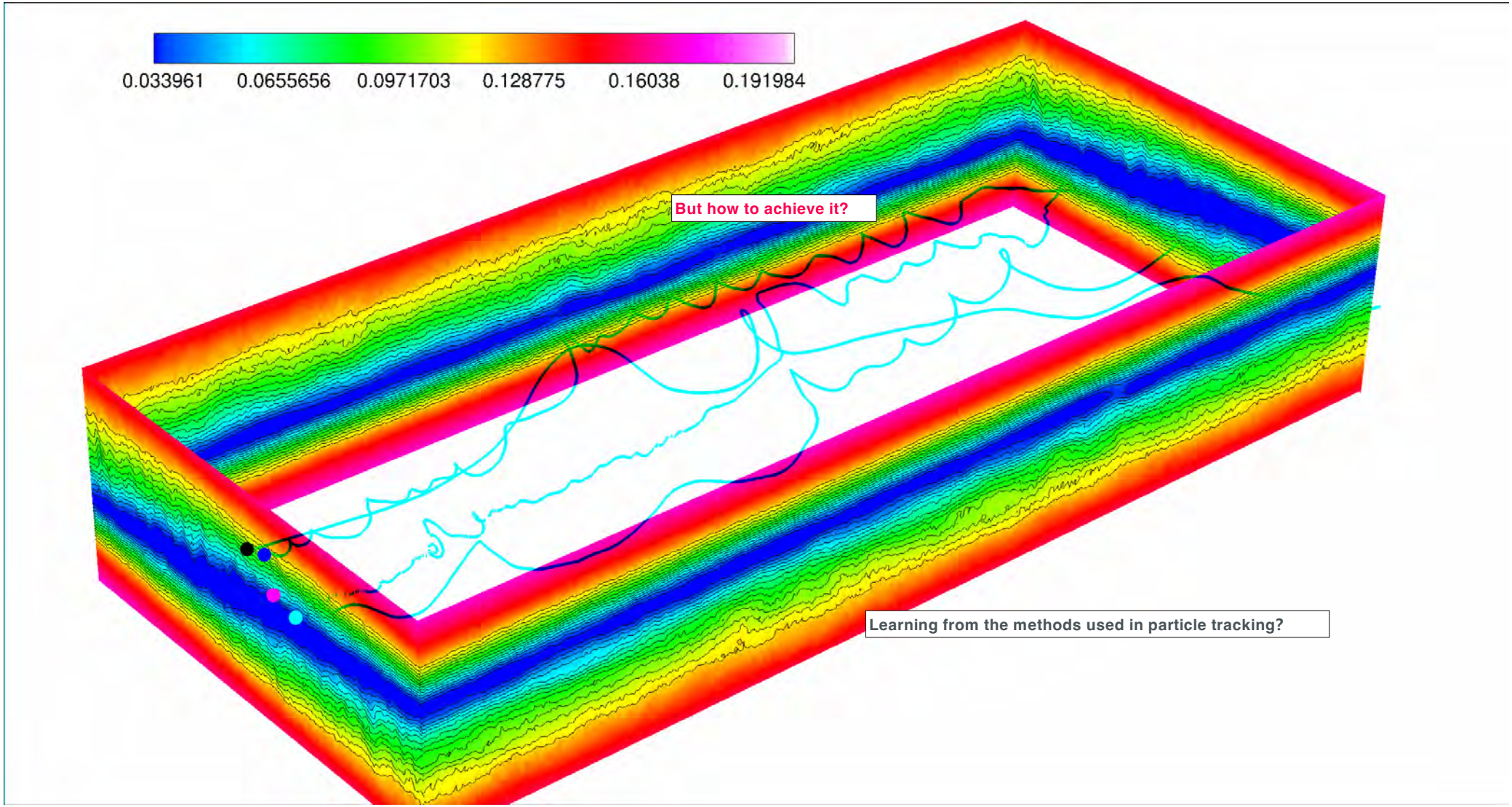

RHPIC-LBM validation

3D turbulence acceleration model II-B&U decoupled &Instabilities

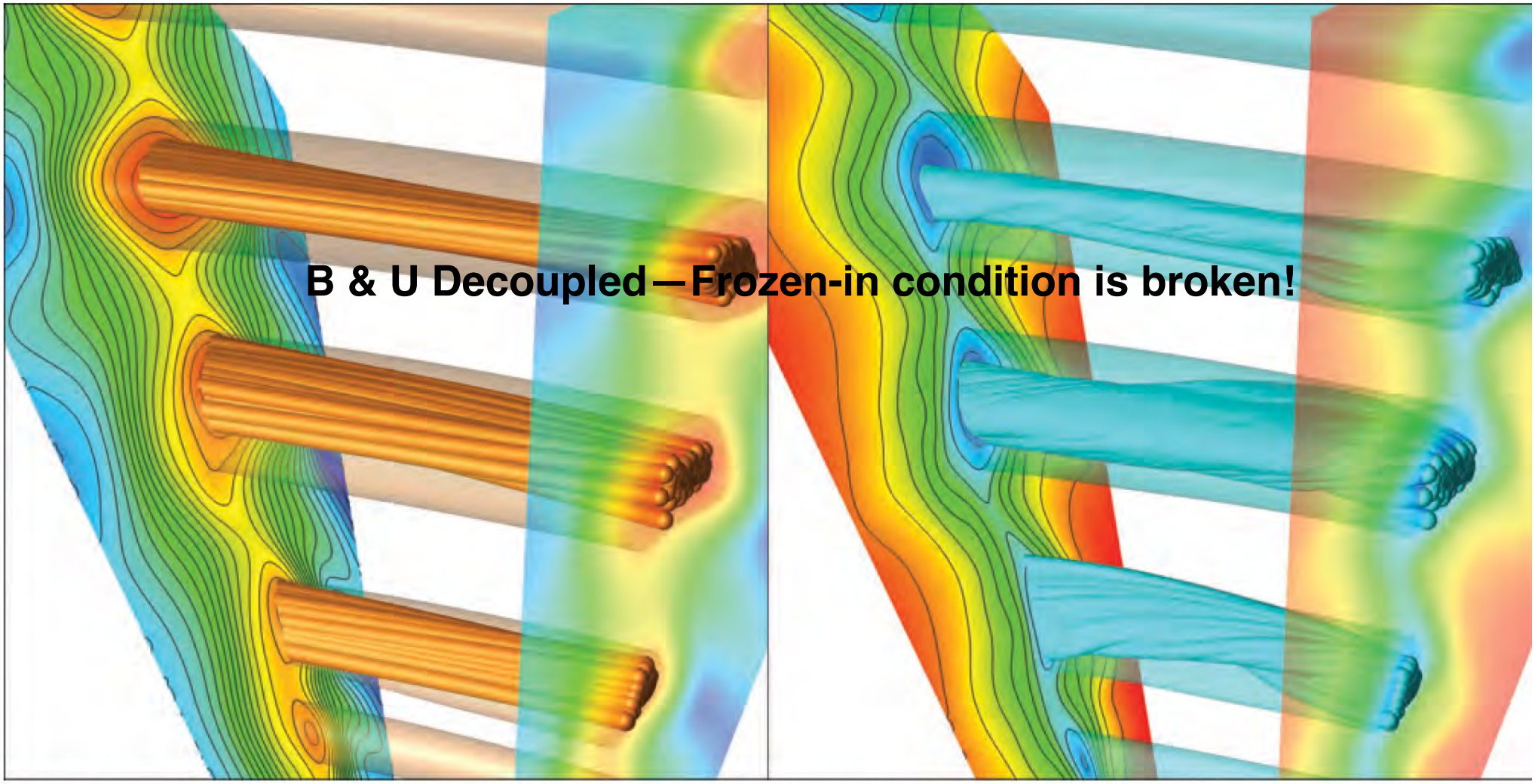

RHPIC-LBM validation

3D turbulence acceleration model II-B&U decoupled &Instabilities

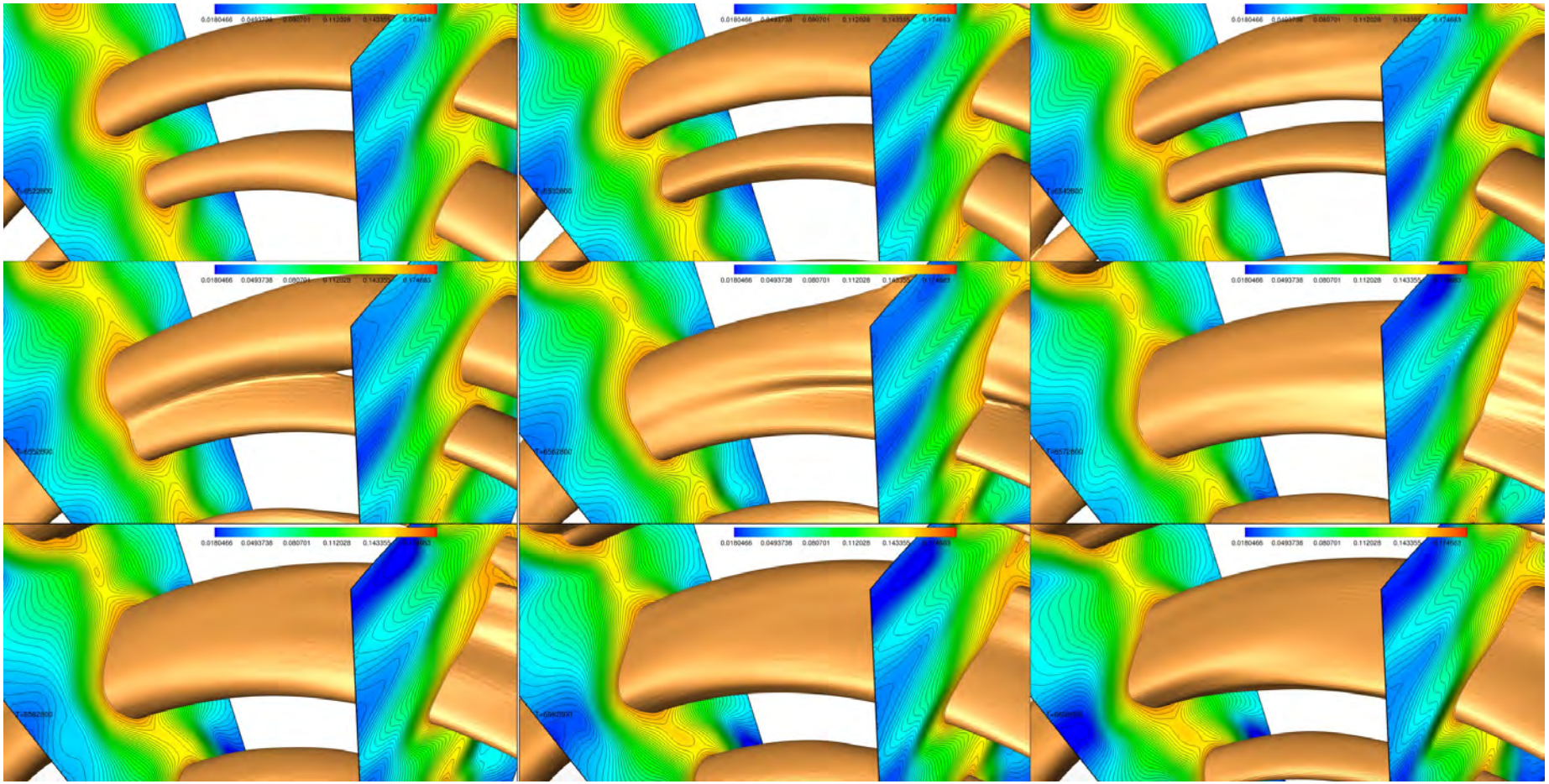

The cross-section of the multi-loops (MFLs/PFLs), d, is the approximately circular, ellipse or long ellipse cross-section with the equivalent diameter equal to the width between the upper and lower boundaries of the loops (MFLs/PFLs), vary from 0.6 Mm to 2 Mm (1 arcsec ~ 3 arcsecs) and the corresponding peak densities from n to 4n

3D turbulence acceleration model II-B&U decoupled &Instabilities

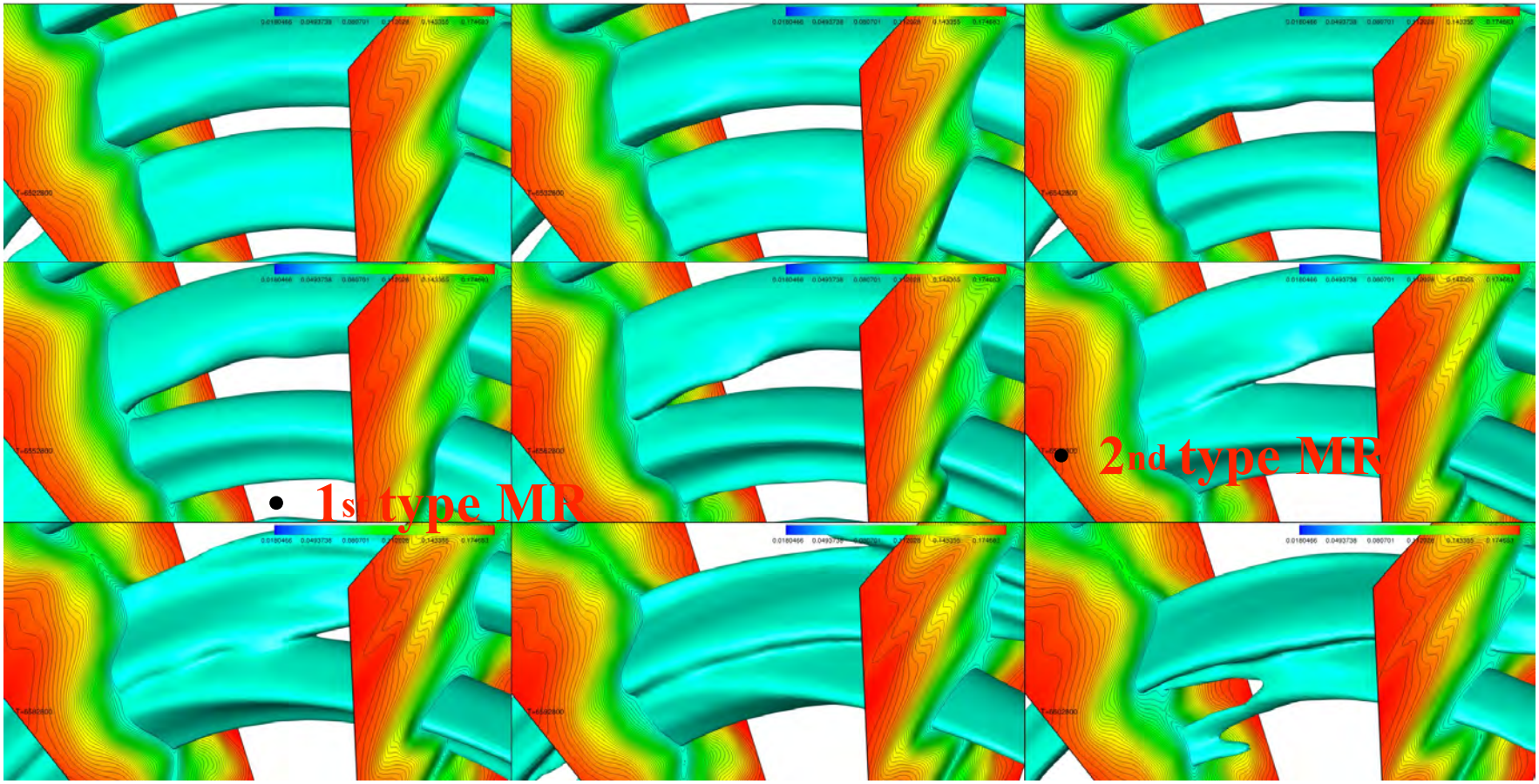

The cross-section of the multi-loops (MFLs/PFLs), d, is the approximately circular, ellipse or long ellipse cross-section with the equivalent diameter equal to the width between the upper and lower boundaries of the loops (MFLs/PFLs), vary from 0.6 Mm to 2 Mm (1 arcsec ~ 3 arcsecs) and the corresponding peak densities from n to 4n

RHPIC-LBM validation

3D turbulence acceleration model II-B&U decoupled &Instabilities

- **The interaction of loops (MFLs/PFLs) decreases with height increase,**

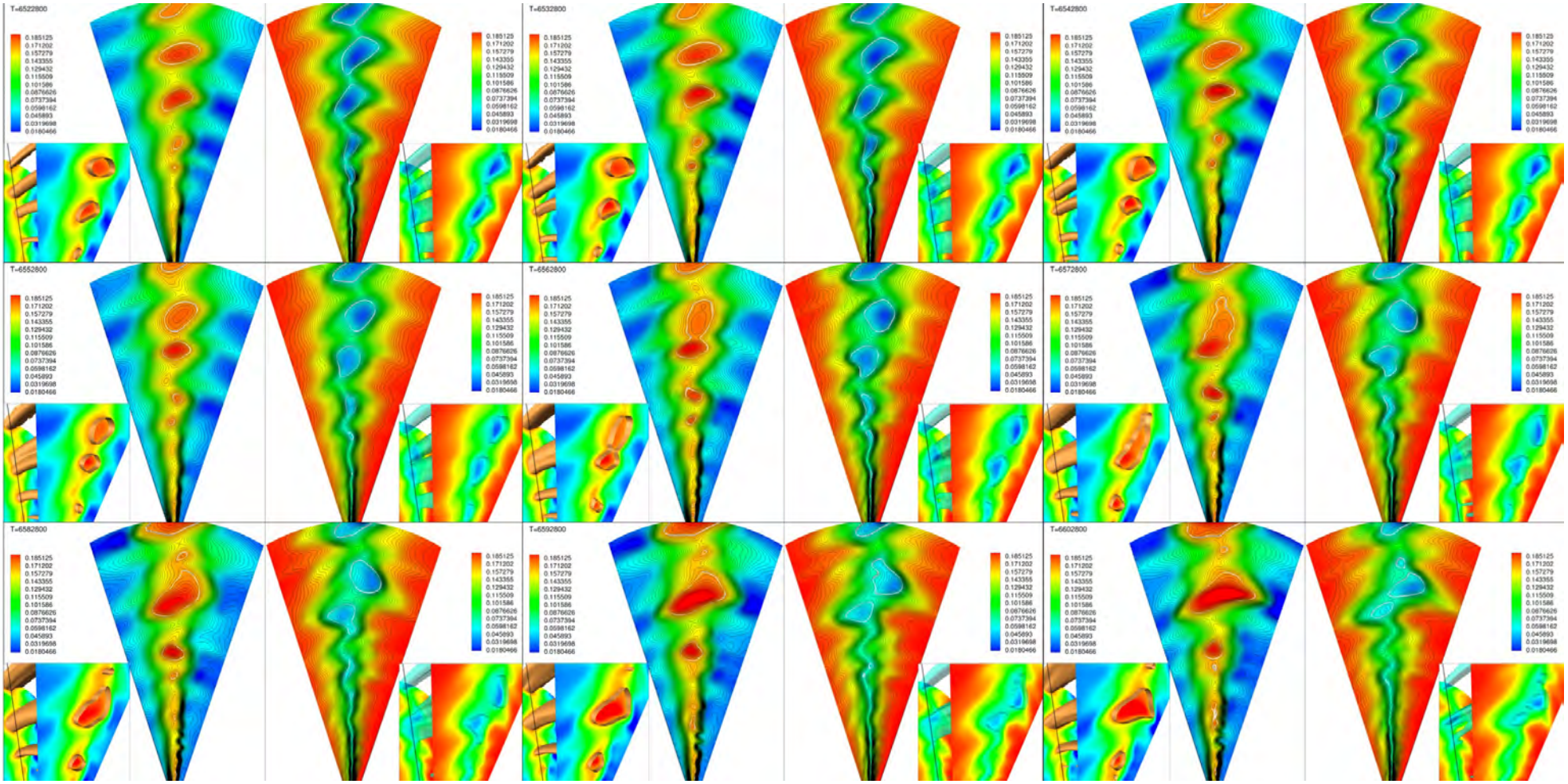

3. Application (Events Study)

3D turbulence acceleration model [source and origin, proton, 3He rich]

Source and Origin

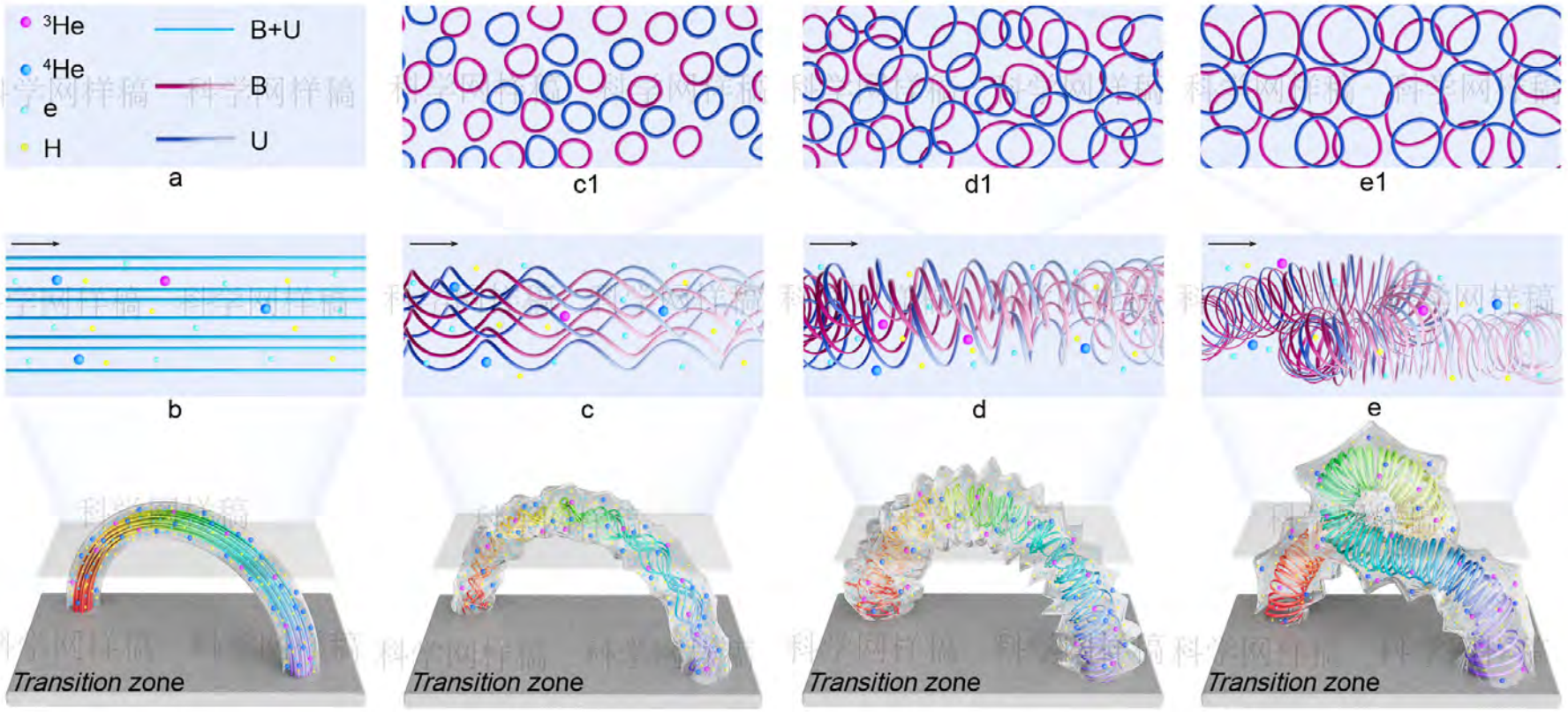

Source and Origin

Turbulence on the top of loop (Twisted Flux Rope wrapping and unwrapping)

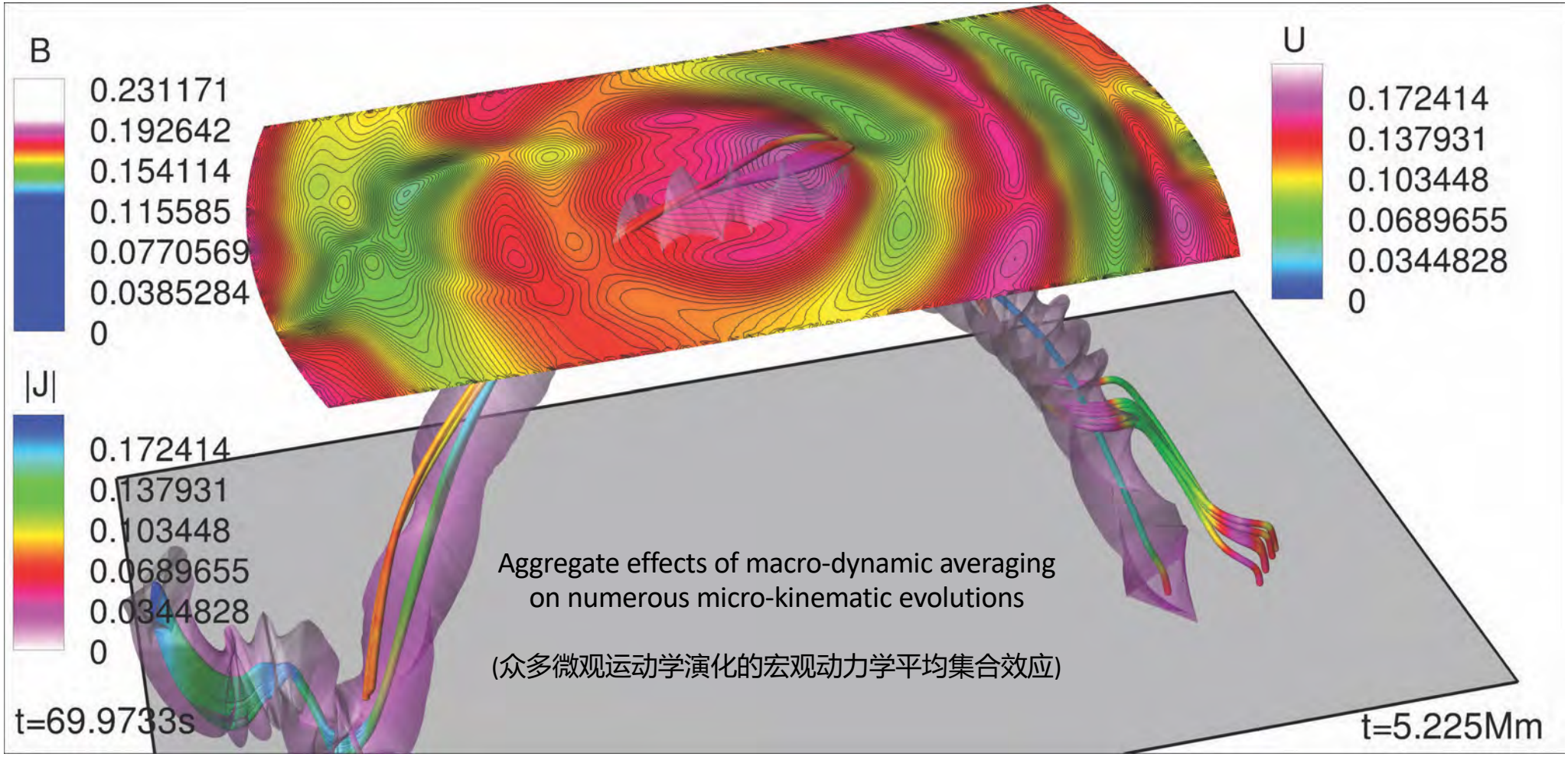

Source and Origin

Turbulence on the top of loop (Twisted Flux Rope wrapping and unwrapping)

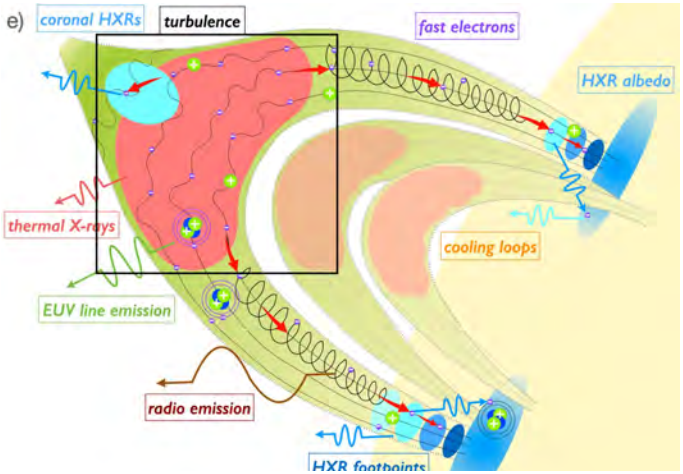

Turbulence _Twisted Flux Rope

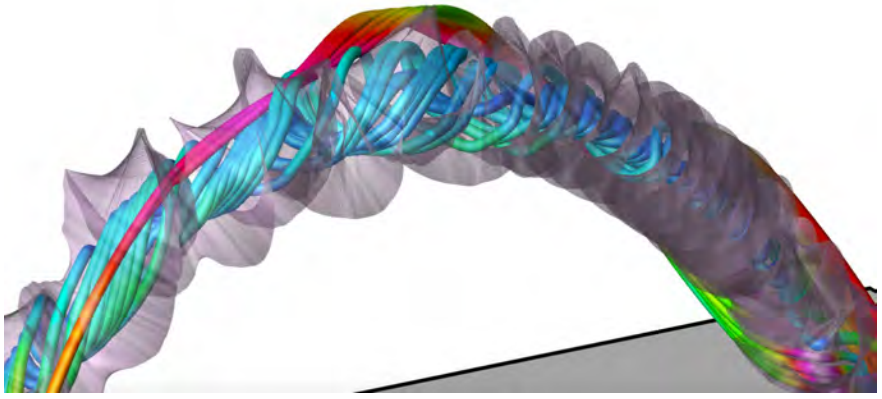

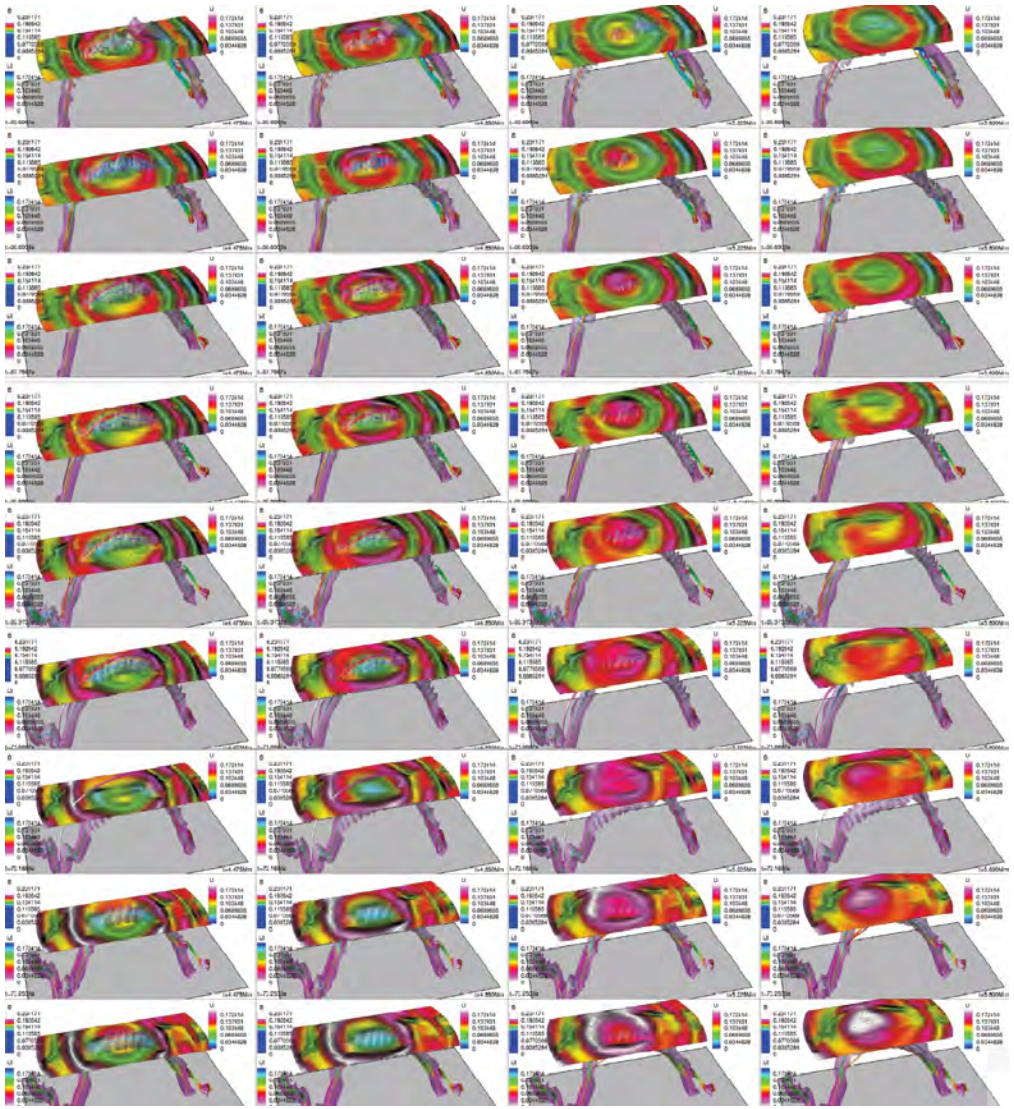

Source and Origin 3D turbulence acceleration model-Source and origin (Proton &electron)

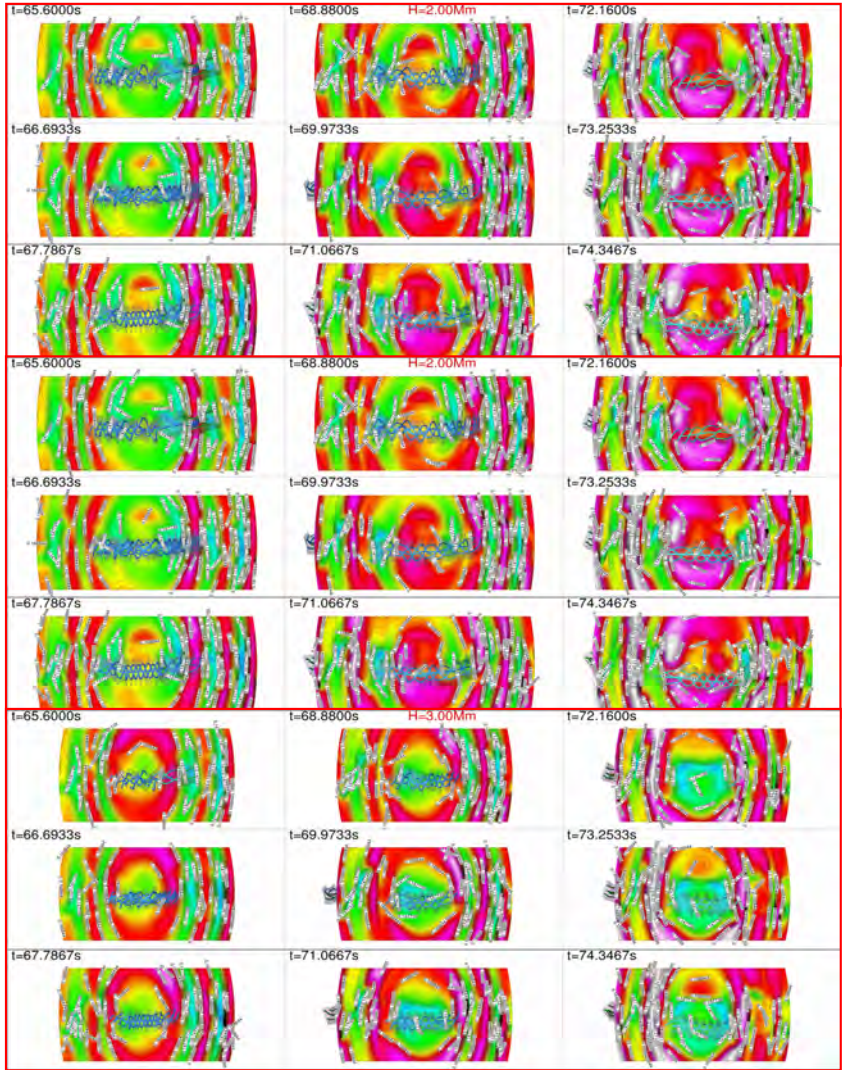

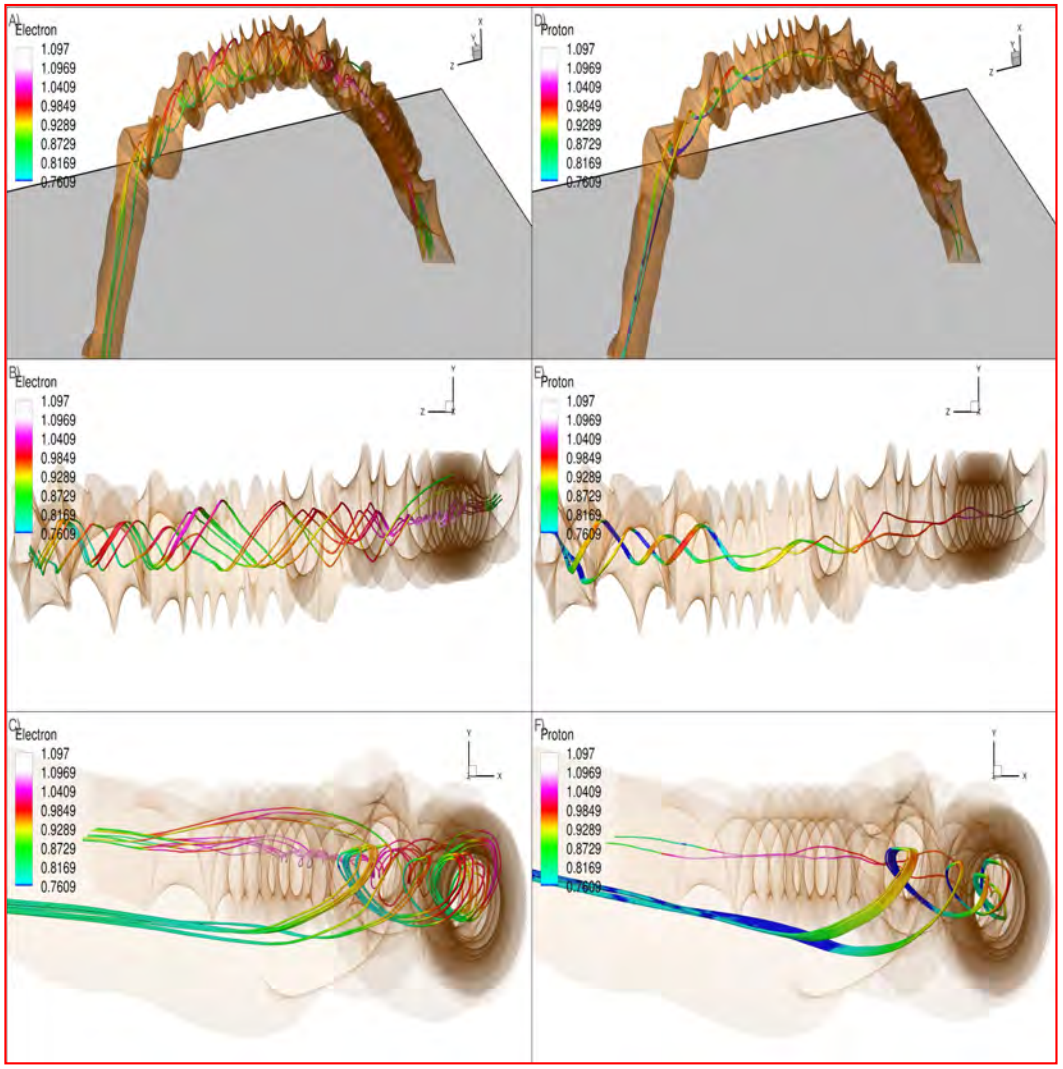

Source and Origin 3D turbulence acceleration model-Source and origin (Proton &electron)

$m_p/m_e = 1836 \quad m_e = 1$

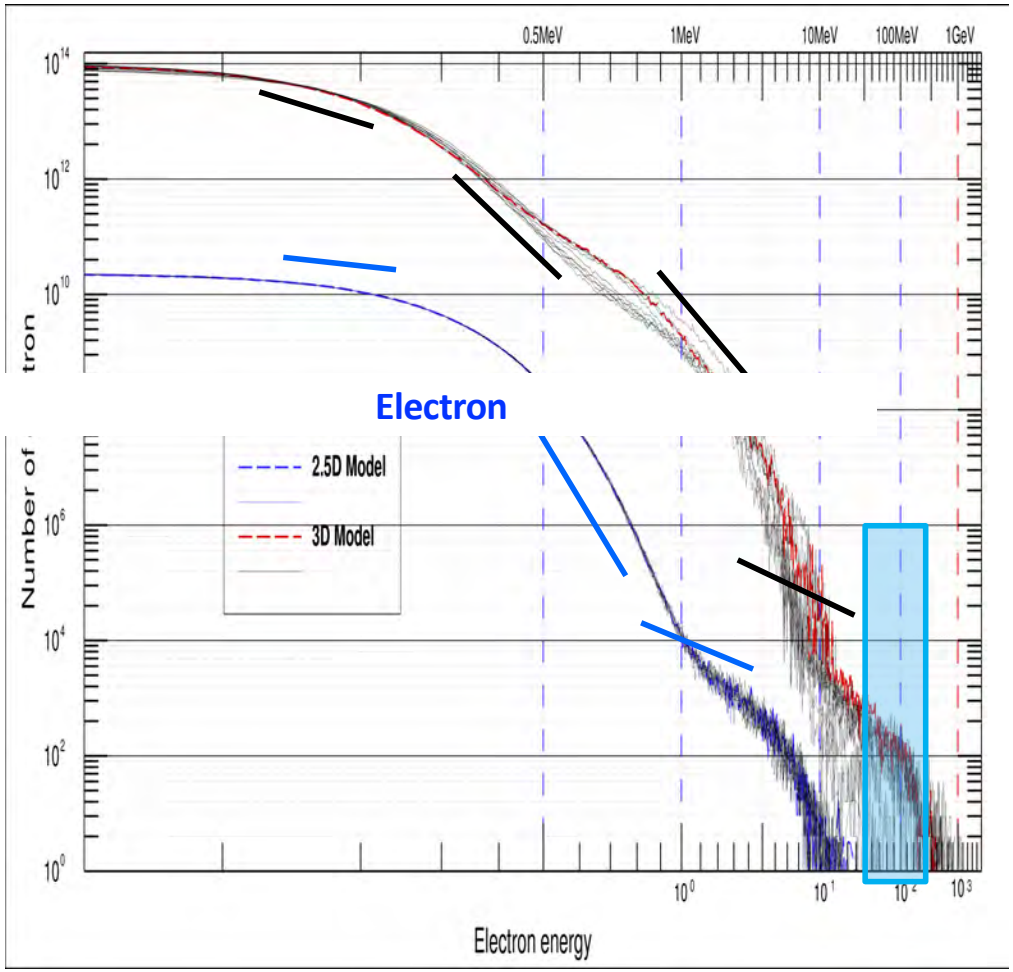

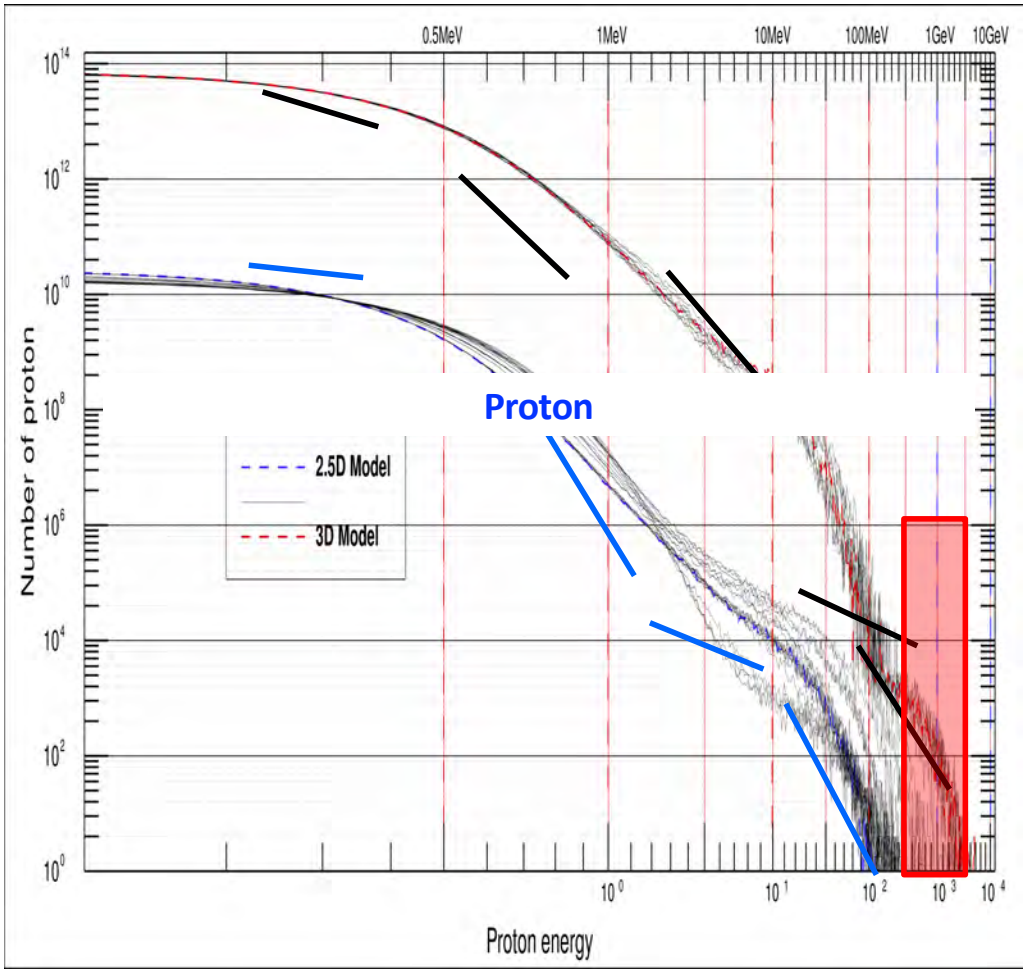

2.D vs 3D turbulence acceleration plus turbulence-induced TVD and TRD

Source and Origin 3D turbulence acceleration model-Source and origin (Proton &electron)

Conclusion

The results show that protons and electrons could be efficiently accelerated simultaneously through the nonlinear resonant wave-particle interaction in the diffusion region, and the interaction of helical magnetic structure leads to efficient energization of electrons, shown as follows:

1. A new nonlinear resonant wave-particle acceleration mechanism in the interaction of helical magnetic structure in large-scale CME/Flare current sheets proposed in solar eruption. The original acceleration model assumed helical magnetic structure evolution in the cross-scaling coupling are separated independent process, which is essential in the helical magnetic structure coalescence and growth process.

2. The multi-component acceleration mechanism and the quantitative relationship between solar flares-CME events and GeV-level SEPs events with the data-driven RHPIC-LBM algorithm and parallel code. We hope this provides a new understanding of SEP sources and origins.

3. We found the Langmuir turbulence acceleration (LTA) through the nonlinear resonant wave-particle interaction by tracking the trajectories and analyzing the energy spectrum of energetic protons and electrons. LTA is an independent acceleration mechanism similar to shock acceleration. Still, it is much more efficient than shock acceleration, indicating that large-scale reconnection is a good candidate for the efficient acceleration of protons and electrons in solar eruption. In summary, we anticipate identifying the source and origin of SEPs as a critical point for understanding the relationship between SEPs acceleration and explosive energetic electrons observed in the solar flares during MHD Alfven turbulence translates into Kinetic Alfven turbulence progress and provides a tool for extreme space weather SEPs forecasting.

Aggregate effects of macro-dynamic averaging on numerous micro-kinematic

Source and Origin

3D turbulence acceleration model-Source and origin (3He rich)

$m_n/m_e = 1836 \quad m_p/m_e = 1836 \quad m_{^3He} = 2m_p + m_n = 5508 \quad m_{^4He} = 2m_p + 2m_n = 7344 \quad m_e = 1$

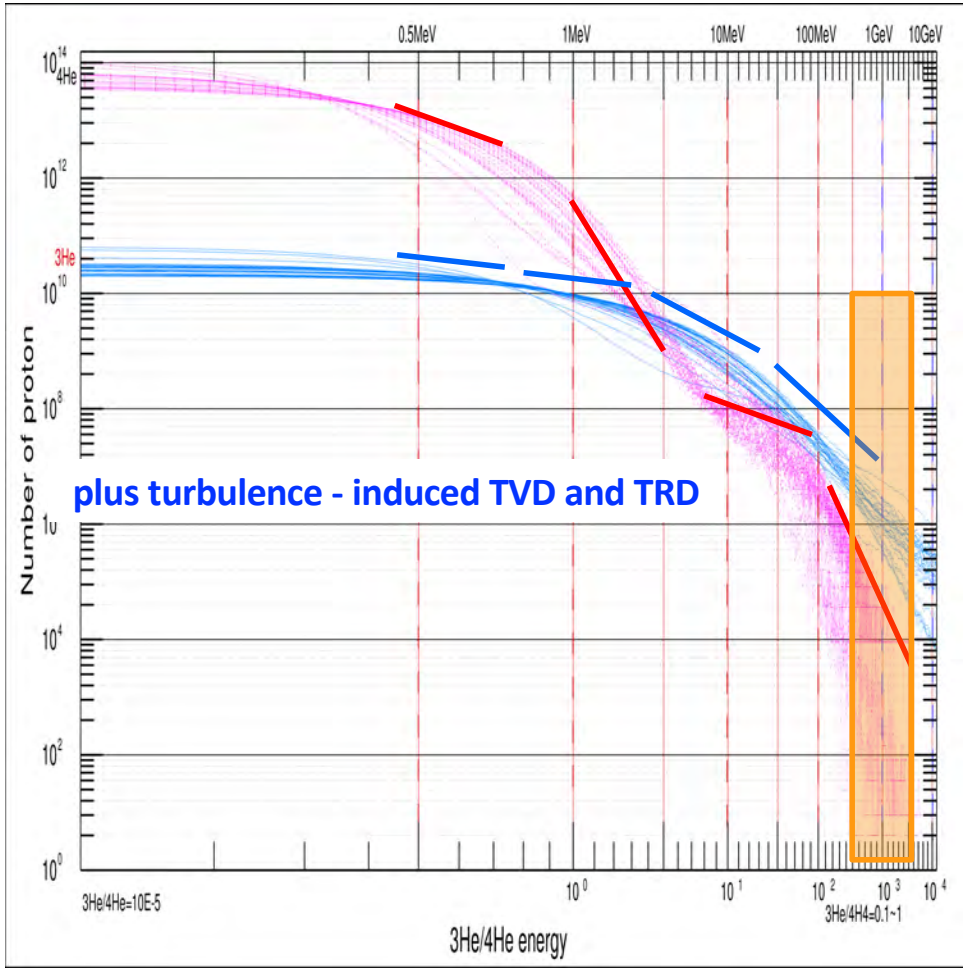

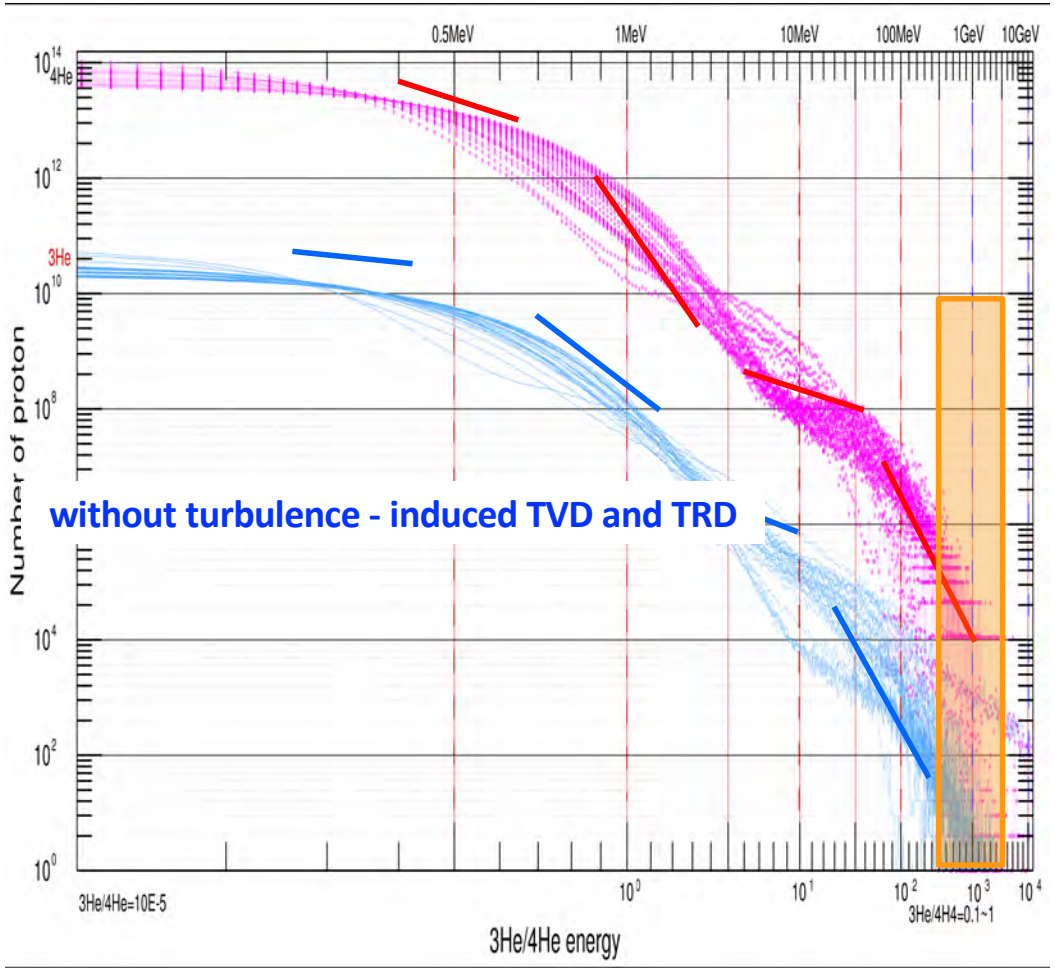

Wave-particle interaction turbulence acceleration

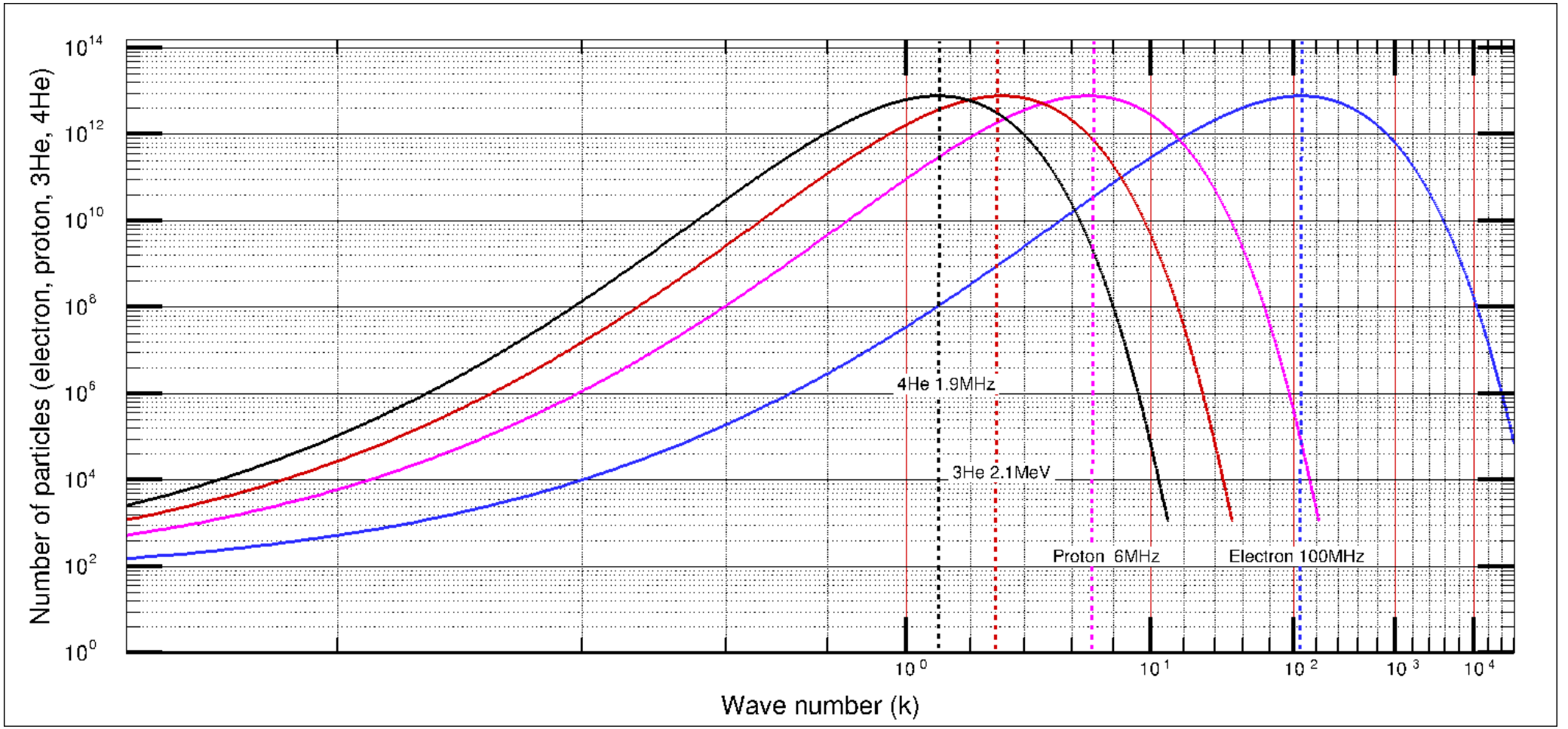
Number of particles (electron, proton, 3He, 4He)
10^{14}
10^{12}
10^{10}
10^{8}
10^{6}
10^{4}
10^{2}
10^{0}
4He 1.9MHz
3He 2.1MeV
Proton 6MHz
Electron 100MHz
10^{0}
10^{1}
10^{2}
10^{3}
10^{4}
Wave number (k)

PSP、Solar Orbiter Observational data

Electrons and Ions are accelerated out of thermal equilibrium due to magnetic reconnection event

Electrons

1. 10^{36} per sec accelerated for ~100 s
2. Maximum energy ~ 100 MeV

Ions

1. 10^{35} per sec accelerated for ~100 s
2. Maximum energy ~ 10 GeV

Nariaki V. Nitta讨论“三尺度五阶段耦合湍流”对3He丰度之谜如何更好解释问题

Irina Kitiashvili&Tamar Ervin,Chadi Salem,Ace Stratton, Meredith Wieber等讨论了PSP观测质子10GeV能级/电子100MeV与RHPIC-LBM模拟合作

Patrick antolin, Stephane Regnier, Yash Saneshwar, Eamon Scullion等讨论了RHPIC-LBM自主知识产权软件合作

Source and Origin

3D turbulence acceleration model-Source and origin (3He rich)

Conclusion

To 3He-rich (3He/4He ratio >0.01) events showing up to 10,000-fold abundance enhancement in the pulse solar hurricanes have been a puzzle for more than 60 years since their discovery.

In this work, based on the statistical physics theoretical model combined with the filter theory of turbulence, we investigate the interaction of 3He/4He, proton, and electron particles acceleration process by the actual ratio of the proton mass to the electron mass and turbulence resistivity & viscosity item under fully coupled kinetic-dynamic continuous scale (instead of the micro-kinetic and macro-dynamic scale separated independent process) on the supercomputer with relativistic hybrid particle-in-cell & lattice-Boltzmann (RHPIC-LBM) innovative algorithm and parallel code.

1. We have discovered a new independent turbulence, the wave-particle interaction acceleration. This novel nonlinear acceleration mechanism is distinct from the current turbulence acceleration mechanism, including 1st and 2nd fermi acceleration; it is more efficient at the GeV level than the shock wave acceleration mechanism. This finding has profound implications for our understanding of space weather disasters and the safety of space orbiters.

2. Tracking the trajectories and analyzing the energy spectrum of energetic 3He/4He allows protons and electrons to be efficiently accelerated simultaneously through the nonlinear resonant wave-particle interaction in the diffusion region. Due to the different proton-to-electron mass ratios, more 3He/4He particles have reached the GeV level.

3. We found that Langmuir turbulence acceleration (LTA) through the nonlinear resonant wave-particle interaction prefers to accelerate particles with a resonance frequency of 3He, which lead is much more efficient than 4He particles.

Aggregate effects of macro-dynamic averaging on numerous micro-kinematic

4. Summary and Future work

Science point:

1. **What is the difference between shock wave acceleration(turbulence acceleration;1st Fermi, and 2nd Fermi) and wave-particle interaction acceleration**
2. **Other heavy particles**
3. **Different ionization states**

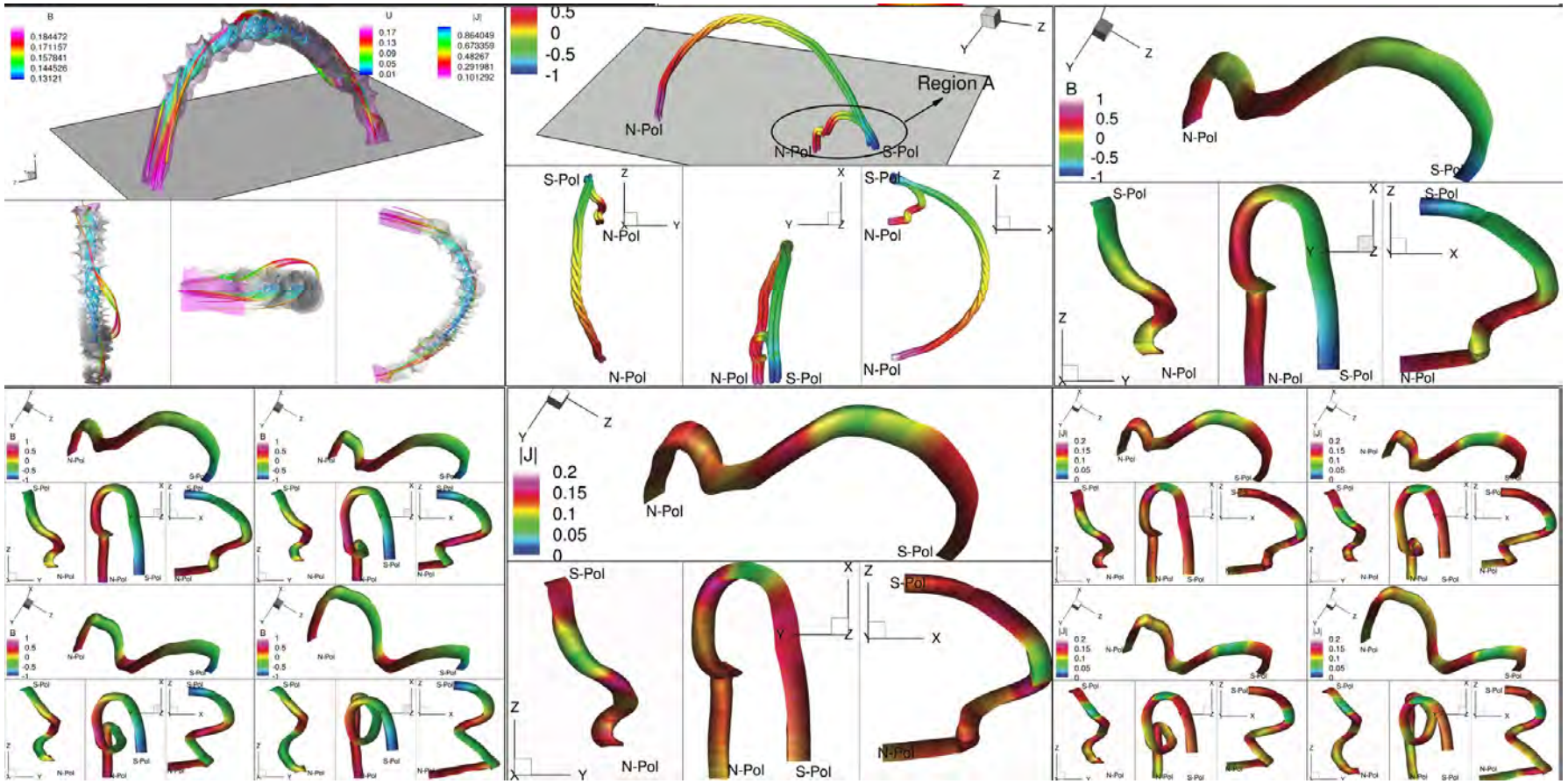

The 12th International Workshop on GPU, MIC, Big Data and Cloud Computing Solutions to Multi-Physics Problems

2025CGU http://www.cgu.org.cn/cugs/?q=node/158&page=3, 2025.10.18-22，Chengdu

中国地球科学联合学术年会

Annual Meeting Of Chinese Geoscience Union(CGU)

CGU-2025 http://www.cgu.org.cn October 18-22 Chengdu

(2) High-Performance Computing Space-Weather/Electromagnetic-Environment Disasters

Conveners:Bojing Zhu,Yongbing Li,Wu Wang,Yonghui Li,Henry Tufo

The plasma in the panoramic view Sun-Earth system includes the Earth's outer core plasma that the main material general the geomagnetic filed, the upper atmosphere and the Earth's magnetosphere environment that protect the high-energy radiation and seriously affects human microwave communications, and the flare/CME plasma that the main reason for Earth's electromagnetic environment.Space-weather/electromagnetic-environment disasters can cause significant catastrophic damage to in-orbit spacecraft, astronauts, deep space exploration, and ground-based electrical facilities.it is identified as a priority area among the five key scientific themes outlined in the National Mid- and Long-term Plan for Space Science in China (2024–2050).It will be held in conjunction with the 12th International Workshop on GPU, MIC, Big Data,Cloud Computing, and AI. Conference topics:①Computational space electromagnetic environment and associated fields;②Computation space weather and associated fields;③ Other related topics.

In memory of **Prof. Dr. David Alexander Yuen**, who passed away in 2023, for his invaluable support in my academic research career.

Global Astro and Space Science Congress (GASSC2026), taking place **in London, UK, from May 04–05, 2026**

Global Astro & Space Science Congress, where Astro & Space Science minds unite to shape the future. To discover ground-breaking research, connect with top professionals, and explore innovations transforming Astro & Space Science

https://globalastrospacesciencecongress.com/core-committee